Assessment framework to predict sensitivity of marine calcifiers to ocean alkalinity enhancement – identification of biological thresholds and importance of precautionary principle

Nina Bednaršek[1], Hanna van de Mortel[2], Greg Pelletier[3,☆], Marisol García-Reyes[4], Richard A. Feely[5], and Andrew G. Dickson[6,☆]

[1]Cooperative Institute for Marine Ecosystem and Resources Studies, Hatfield Marine Science Center, Oregon State University, 2030 SE Marine Science Drive Newport, OR 97365, USA
[2]HvdMortel Consulting, Utrecht, the Netherlands
[3]Washington Department of Ecology, Olympia, 300 Desmond Dr SE, WA 98503, USA
[4]Farallon Institute, 101 St. Suite Q, Petaluma, CA 94952, USA
[5]NOAA Pacific Marine Environmental Laboratory, Seattle, WA 98115, USA
[6]University of California at San Diego, Scripps Institution of Oceanography, 9500 Gilman Drive, La Jolla, CA 92093, USA
☆retired

Correspondence: Nina Bednaršek (nina.bednarsek@oregonstate.edu)

Abstract. Ocean alkalinity enhancement (OAE), one of the marine carbon dioxide removal strategies, is gaining recognition in its ability to mitigate climate change and ocean acidification (OA). OAE is based on adding alkalinity to open-ocean and coastal marine systems through a variety of different approaches, which raises carbonate chemistry parameters (such as pH, total alkalinity, aragonite saturation state) and enhances the uptake of carbon dioxide (CO_2) from the atmosphere. There are large uncertainties in both short- and long-term outcomes related to potential environmental impacts, which would ultimately have an influence on the social license and success of OAE as a climate strategy. This paper represents a synthesis effort, leveraging on the OA studies and published data, observed patterns, and generalizable responses. Our assessment framework was developed to predict the sensitivity of marine calcifiers to OAE by using data originating from OA studies. The synthesis was done using raw experimental OA data based on 68 collected studies, covering 84 unique species and capturing the responses of 11 biological groups (calcifying algae, corals, dinoflagellates, mollusks, gastropods, pteropods, coccolithophores, annelids, crustacean, echinoderms, and foraminifera), using regression analyses to predict biological responses to NaOH or Na_2CO_3 addition and their respective thresholds. Predicted responses were categorized into six different categories (linear positive and negative, threshold positive and negative, parabolic and neutral) to delineate responses per species. The results show that 34.4 % of responses are predicted to be positive ($N = 33$), 26.0 % negative ($N = 25$), and 39.2 % ($N = 38$) neutral upon alkalinity addition. For the negatively impacted species, biological thresholds, which were based on 50 % reduction of calcification rate, were in the range of 50 to 500 $\mu mol\,kg^{-1}$ NaOH addition. Thus, we emphasize the importance of including much lower additions of alkalinity in experimental trials to realistically evaluate in situ biological responses. CE1 The primary goal of the research was to provide an assessment of biological rates and thresholds predicted under NaOH / Na_2CO_3 addition that can serve as a tool for delineating OAE risks. This will help guide and prioritize future OAE biological research and regional monitoring efforts CE2 and will also aid in communicating risks to stakeholders. This is important given the fact that at least some of the current OAE approaches do not always assure safe biological space. With 60 % of responses being non-

neutral, a precautionary approach for OAE implementation is warranted, identifying the conditions where potential negative ecological outcomes could happen, which is key for scaling up and avoiding ecological risks.

1 Introduction

Anthropogenic carbon dioxide (CO_2) emissions have increased at an unprecedented rate and have contributed to global climate change and negative ecological and biogeochemical impacts in the oceans (Feely et al., 2004; Gattuso et al., 2018), to the extent of crossing six different planetary boundaries (Richardson et al., 2023). Oceans play a crucial role in attenuating the increase in atmospheric CO_2 through the absorption of the excess atmospheric CO_2 of roughly a quarter of anthropogenic carbon dioxide (CO_2) emissions, drawing down around 2–$3\,Pg\,C\,yr^{-1}$ in recent decades (Friedlingstein et al., 2022). However, without substantial CO_2 emissions abatement and CO_2 removal strategies, profound repercussions on climate, extreme weather events, and socioeconomic implications will follow. Ocean-based CO_2 removal and sequestration strategies, broadly referred to as marine carbon dioxide removal (mCDR) CE3, are among the proposed CO_2 removal approaches that remove CO_2 and store it for geologically relevant times (National Academies of Sciences, Engineering, and Medicine, 2021). These mCDR approaches only complement CO_2 emission reductions and contribute to the portfolio of climate response strategies needed to meet the global goal of limiting warming to well below $2\,°C$ as established by the Paris Agreement. Various mCDR approaches have unique benefits and costs but differ in their value depending on their state of implementation and whether they act globally and/or locally (Oschlies et al., 2023).

Ocean alkalinity enhancement (OAE) has the potential to mitigate climate change through increasing ocean uptake of CO_2 while simultaneously reversing ocean acidification (OA) and improving marine habitats. Despite mostly being in the concept stage, OAE is viewed with a high level of confidence as to its effectiveness: medium on environmental risk but low on the underlying knowledge base (Eisaman et al., 2023; Gattuso et al., 2021; National Academies of Sciences, Engineering, and Medicine, 2021). One of the major concerns about OAE is large uncertainties in both short- and long-term OAE outcomes related to potential environmental impacts of OAE (Kheshgi, 1995; Bach et al., 2019), especially if OAE were to induce novel conditions in the marine systems that are outside the range of the natural variability, exposing organisms to conditions not experienced in their evolutionary history. The outcome of OAE as a successful climate strategy depends on a thorough and advanced understanding of the impacts of OAE implementation while avoiding or minimizing negative biological effects.

1.1 Leveraging ocean acidification research on marine calcifiers

Increased CO_2 uptake, which initially is absorbed by the ocean as dissolved CO_2, causes a decline in pH, shoaling of the saturation state horizon (Ω_{ar}), and reduced carbonate ion amount content in a process termed ocean acidification (Feely et al., 2004), causing negative consequences to marine biota, especially marine calcifiers, the structure and function of the vulnerable marine ecosystem, and alteration of the carbon cycle. On the other hand, chemical changes induced by OAE are inherently linked to reversing the OA process: increasing pH, shifting carbonate chemistry speciation towards lower aqueous carbon dioxide (pCO_2) and higher carbonate ion (CO_3^{2-}) content, and increasing aragonite saturation state (Ω_{ar}). Such changes could be either within the ranges of the variability of the natural systems to which species are acclimatized or outside them, creating novel conditions for which species might not have developed suitable acclimation strategies. As such, the biological outcomes are, due to their complexity, highly unpredictable.

Scientific progress over the past 30+ years of OA research has offered substantial insights into the biological effects, with the most fundamental outcome being that calcifying organisms would be primarily affected (Riebesell and Gattuso, 2015), with the calcification process being one of the most susceptible pathways, underpinned by species differences in calcification mechanisms (Ries et al., 2009; Ries, 2011; Bach and Mackinder, 2013; Bach et al., 2015; Leung et al., 2022). However, OA focused heavily on investigating biological effects on the higher acidity range of the carbonate chemistry conditions predicted under future scenarios, and most of the studies focused on manipulating the level of pCO_2 rather than alkalinity. This resulted in poor understanding of the biological effects at the higher pH end of the carbon chemistry range (Renforth and Henderson, 2017). Some biological inferences can be made based on the understanding of the physiological mechanisms underlying the calcification mechanisms (Bach et al., 2019), but such insights are not adequate to provide sufficient understanding. Despite the lack of biological data at the upper ranges of pH and Ω_{ar}, this study builds on the premise that previous OA studies could be leveraged for assessment of biological responses under OAE. Comparative experimental work, meta-analyses, and the threshold work (Kroeker et al., 2013; Leung et al., 2022; Bednaršek et al., 2019, 2021b, c) have indicated that even very diverse responses can be grouped into categorical responses.

Calcification is a primary pathway through which organismal sensitivity to OA is expressed. It is directly involved in growth and (abnormal) development across most marine calcifiers, and it indirectly influences susceptibility to predation. As such, calcification can serve as an early warning indicator of stress while also playing a crucial role in the ecological success of numerous marine calcifiers. Stud-

ies have shown that the thresholds for calcification occur at similar pH and saturation state (Ω) values to those affecting energy metabolism processes (Lutier et al., 2022; Bednaršek et al., 2019, 2021b, c). Furthermore, calcification is directly linked to carbon export, which has significant biogeochemical implications that may influence the efficiency of OAE. This study aims to systematically assess the calcification responses of various species under predicted conditions following carbonate-based OAE compound addition.

1.2 Complex carbonate chemistry changes induced by various OAE compounds

Various OAE compounds added to the water change carbonate chemistry in a multifaceted way and require complex calculations of a multi-parameter problem. As the values of total alkalinity (TA) and dissolved inorganic carbon (DIC) change, a variety of other parameters (such as pH, CO_3^{2-}, Ω_{ar}, and $p\text{CO}_2$) exhibit approximately linear relationships, with slopes that vary along these lines (see Fig. 1). This means that if TA and DIC vary in proportion to one another, then the values of these displayed parameters hardly change at a particular salinity, temperature, and pressure. With TA, DIC, and the hydrographic conditions (salinity, temperature, and pressure), one can constrain the carbonate system. Our method requires us to have *one* variable constraining the entire carbonate system. TA and DIC have the benefit that they can both be directly measured with high precision and accuracy or calculated from other carbonate parameters. They are also both directly linked to OAE, as we are enhancing the TA which then allows DIC to increase over time due to the gradual uptake of atmospheric CO_2.

To demonstrate the changes of the carbonate system in the experimental system, Fig. 1 shows the changes in carbonate parameters with the addition of two OAE compounds, i.e., NaOH (solid line) and Na_2CO_3 (dashed line) to seawater. When NaOH is added, only TA increases, and when Na_2CO_3 is added, TA and DIC increase at a 2 : 1 ratio. This results in corresponding changes in pH (Fig. 1a), Ω_{ar} (Fig. 1b), and $p\text{CO}_2$ (Fig. 1c) and shows how much of a change is required to bring the system back to equilibrium with respect to the atmosphere.

1.3 Testable conceptual framework based on the existing OA studies

Based on Ries et al. (2009), calcification responses can be categorized into six categories (Fig. 2): linear positive or negative response, threshold positive or negative response (exponential fit), parabolic response, and neutral (no significant) response. We hypothesize that these categories of responses based on ocean acidification data and delineated by Ries et al. (2009) and Ries (2011) could also be applicable to OAE dosing. For this meta-analysis, we have undertaken three steps: first, synthesize carbonate chemistry data at regional and global scales to obtain TA, DIC, and Ω_{ar} correlations; second, conduct a literature review and collect available data from OA literature related to the calcification rate responses across the species of 11 groups of marine calcifiers; and, third, run regression analyses and determine the category of calcification rate response to TA : DIC, further extending it with addition of NaOH and Na_2CO_3.

The most accurate way of predicting the responses to OAE addition is done based on the mechanistic understanding of calcification response to specific carbonate chemistry parameter(s). The hypothesis was that if mechanistic relationships with identified carbonate chemistry driver(s) are available for species, calcification rate under various feasible OAE scenarios can be predicted with greater accuracy and lower uncertainty. We further focused on investigating whether the empirical results were consistent with mechanistic calcification predictions for a few selected species for which the mechanisms were known.

Here, we demonstrate the TA : DIC relationship with calcification rates and show the application for the TA : DIC thresholds beyond which the responses become negative. Ultimately, we synthesize which calcifying species or groups are predicted to benefit or lose due to OAE and what constitutes a species-specific safe operating space related to OAE. We also delineate what experiments are most urgently needed to fill in critical knowledge gaps before massive OAE field implementation can be considered.

2 Methodology

2.1 Literature review of data on marine calcification impact by OA

To assess the impact of OAE on a range of marine calcifiers, we used existing studies on marine species calcification response to OA that had aligned raw biological (calcification rate) data along with corresponding carbonate chemistry. We searched within Scopus, Web of Science, and PubMed and used datasets that were archived in NCEI, OA-ICC, and Pangaea. Through personal correspondence, we have additionally contacted the lead authors of the studies whose data are not or are insufficiently archived. Searches for biological datasets relating to calcification rate and corresponding carbonate chemistry were conducted through November 2023, encompassing 68 existing studies. The aim was to cover a wide range of calcifying organisms across various functional groups and 84 species. For several functional groups, data were easy to find (algae, coccolithophores, corals, foraminifera, mollusks, and dinoflagellates), so no new studies were added after 10 to 15 studies were found. Seven studies were found for pteropods, five for gastropods, four for echinoderms, three for crustaceans, and one for annelids. When reviewing the literature, we included data from OA experimental studies related to the physical–chemical pa-
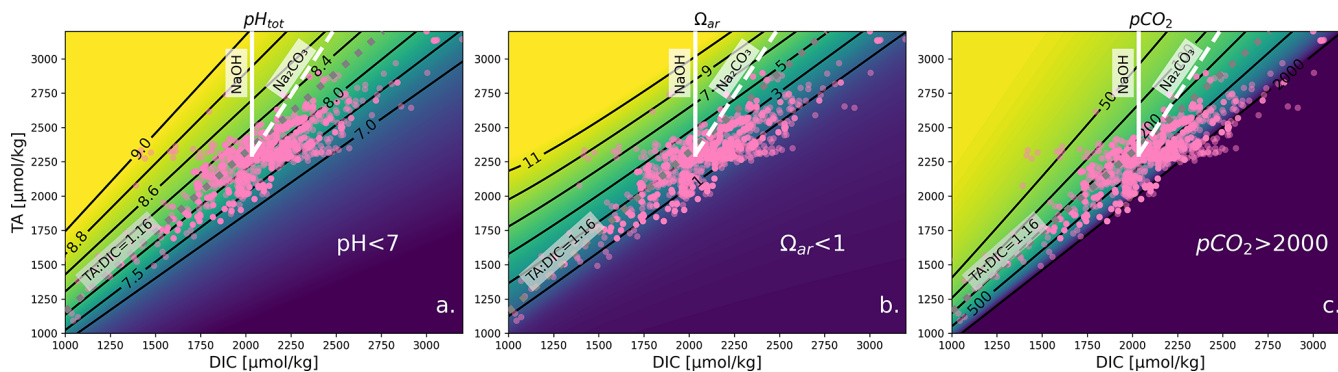
Figure 1. The effect of changes in TA and DIC on the properties of seawater ($S = 34.68$, $T = 16\,°C$, $[SiO_2] = 50\,\mu mol\,kg^{-1}$, $[PO_4^{3-}] = 0.5\,\mu mol\,kg^{-1}$, TA $= 2303\,\mu mol\,kg^{-1}$, DIC $= 2034\,\mu mol\,kg^{-1}$), adapted from Schulz et al. (2023). Pink dots represent experimental TA and DIC data used in our synthesis. Subfigures show pH_T, Ω_{ar}, and pCO_2 (in µatm). Calculations were carried out with the Python version of CO2SYS (Humphreys et al., 2022) using the stoichiometric dissociation constants for carbonic acid from Sulpis et al. (2020), for sulfuric acid by Dickson (1990), and for total boron from Uppström (1974). The solid white line indicates the effect of adding NaOH, and the dashed white line indicates the effect of adding Na_2CO_3. This grouping of lines can be translated so that its initial position moves elsewhere to visualize different initial conditions. Note that at TA < 1000 and DIC $< 500\,\mu mol\,kg^{-1}$, the isolines are no longer straight when considering Ω_{ar}; however, such conditions are rare in the ocean and not widely applicable. The same contour plot utilizing GLODAP data plotted instead of experimental data is shown in Fig. S1.

rameters (temperature, salinity, TA, DIC) and biological data related to calcification rate.

2.2 Use of TA : DIC instead of Ω_{ar} or pH

Understanding the change in carbonate chemistry upon al-
5 kalinity addition is essential for biological experimentalists who are conducting biological assessments to report on the effects of OAE. However, complex changes in carbonate chemistry induced by alkalinity addition are not intuitive or straightforward; in fact, they are multi-parameter problems
10 that require complex carbonate chemistry calculations. Using the TA : DIC ratio is a more practical way of looking at the impacts of the OAE treatment instead of using a single carbonate parameter because of the high degree of correlation between TA : DIC and other carbonate system parame-
15 ters (see Fig. 1).

With TA, DIC, and the hydrographic conditions (salinity, temperature, and pressure), one can fully constrain the carbonate system. Our method allows *one* variable constraining the entire carbonate system. TA and DIC have the benefit
20 that they can both be directly measured or calculated from other carbonate and physical parameters. They are also both directly linked to OAE, as we are enhancing the TA, which then allows DIC to increase over time due to the gradual uptake of atmospheric CO_2 (Fig. 1 shows the changes in the
25 carbonate chemistry system upon NaOH and Na_2CO_3 addition).

Our focus was on streamlining the process of expressing experimental results and subsequently reporting responses, with the goal of reducing the multi-parameter complexity
30 into a single-parameter simplification. This step reduces mul-

tiple degrees of freedom into just two, i.e., TA and DIC, with the ratio allowing us to consider this as a one-parameter problem. As such, TA : DIC is a simplistic and convenient way of describing the system, where we only need to understand the change in TA and DIC ratio, which is feasible
35 for every OAE compound added to the experimental system. In addition, TA : DIC is also the best approximation for the CO_3^{2-} concentration. The insights from multiple biological experimental studies show that the CO_3^{2-} concentration is the representative driver of the calcification process for multiple
40 calcifying groups, although not all, compared to Ω_{ar}, which represents an empirical approximation based on a number of physical and chemical parameters. Furthermore, by using TA : DIC, we do not have to choose a particular parameter to describe the changes in calcification. It could also work for
45 the species in which other parameters drive the calcification, e.g., bicarbonate in autotrophic species, Ω_{ar} in bivalves, and H^+ flux in foraminifera. In that way, we standardize all the parameters that would otherwise influence the carbonate system and come up with a more uniform way to express the ex-
50 perimental conditions, which would then be useful for easier comparisons among the conducted experiments. For the ease of comparing TA : DIC with pH and Ω_{ar}, we refer the reader to Table S1 and Fig. S2.

2.3 Experimental biological and biogeochemical data   55

Based on the collected data, the range of pH and Ω_{ar}, experimental conditions used, and their TA : DIC relationship was determined (Fig. S2 and Table S1). Most studies covered pH conditions from 7.5 to 8.5 and Ω_{ar} from < 1.0 to values up to 5.0, with a few studies increasing pH up to 9 and exceed-   60

Table 1. The summary of all the OA studies from which the chemical and biological data were collected, including the name of the species and group and the accompanying calcification rate unit. The response for each species rate group was determined by the regression with the lowest p value, where the p value was smaller than 0.05. We also include the p value, goodness of fit (R^2), and root mean square error (RMSE). Non-significant responses are categorized as having a "neutral" response. The type of response (linear positive or negative, threshold positive or negative, parabolic, and neutral) is indicated, as well as whether this response is positive (Pos), negative (Neg), or neutral (Neut).

Studies* TSI	Group	n	Species	Rate unit	Response	Pos/Neg/Neut	p value	R^2	RMSE
Vásquez-Elizondo et al. (2016)	Algae	4	*Amphiroa tribulus*	$mmol\ m^{-2}\ h^{-1}$	Neutral	Neutral			
Sinutok et al. (2011)	Algae	16	*Halimeda cylindracea*	$mmol\ h^{-1}$	Neutral	Neutral			
Comeau et al. (2013)	Algae	71	*Halimeda macroloba*	$mmol\ g^{-1}h^{-1}$	Parabolic	Negative	0.0127	0.1200	0.0028
Meyer et al. (2015)	Algae	24	*Halimeda macroloba*	$mmol\ m^{-2}\ h^{-1}$	Neutral	Neutral			
Sinutok et al. (2011)	Algae	16	*Halimeda macroloba*	$mmol\ h^{-1}$	Parabolic	Negative	0.0108	0.5000	0.0001
Comeau et al. (2013)	Algae	62	*Halimeda minima*	$mmol\ g^{-1}h^{-1}$	Neutral	Neutral			
Meyer et al. (2015)	Algae	24	*Halimeda opuntia*	$mmol\ m^{-2}\ h^{-1}$	Linear +	Positive	0.0080	0.2800	0.0222
Comeau et al. (2013)	Algae	72	*Hydrolithon reinboldii*	$mmol\ g^{-1}h^{-1}$	Linear +	Positive	0.0053	0.1100	0.0026
Cornwall et al. (2018)	Algae	23	*Hydrolithon reinboldii*	$mmol\ m^{-2}\ h^{-1}$	Neutral	Neutral			
Comeau et al. (2013)	Algae	72	*Lithophyllum flavescens*	$mmol\ g^{-1}h^{-1}$	Neutral	Neutral			
Johnson et al. (2021)	Algae	420	*Lithophyllum* sp.	$mmol\ g^{-1}h^{-1}$	Linear +	Positive	0.0000	0.1000	0.1136
Vásquez-Elizondo et al. (2016)	Algae	4	*Lithothamnion* sp.	$mmol\ m^{-2}\ h^{-1}$	Neutral	Neutral			
Monserrat et al. (2022)	Algae	62	*Neogoniolithon brassica-florida*	$mmol\ m^{-2}\ h^{-1}$	Neutral	Neutral			
Ries et al. (2009)	Algae	42	*Neogoniolithon* sp.	$mmol\ g^{-1}h^{-1}$	Parabolic	Negative	0.0000	0.4100	0.0003
Vásquez-Elizondo et al. (2016), Comeau et al. (2018)	Algae	26	*Neogoniolithon* sp.	$mmol\ m^{-2}\ h^{-1}$	Neutral	Neutral			
Briggs and Carpenter (2019)	Algae	425	*Porolithon onkodes*	$mmol\ g^{-1}h^{-1}$	Linear +	Positive	0.0010	0.0300	0.8093
Comeau et al. (2018, 2019)	Algae	64	*Sporolithon durum*	$mmol\ m^{-2}\ h^{-1}$	Parabolic	Negative	0.0012	0.2000	0.1704
Ries et al. (2009)	Annelid	41	*Hydroides crucigera*	$mmol\ g^{-1}\ h^{-1}$	Neutral	Neutral			
Fiorini et al. (2011), Langer et al. (2006), Langer and Bode (2011)	Cocco.	14	*Calcidiscus leptoporus*	$mmol\ \#^{-1}\ h^{-1}$	Neutral	Neutral			
*	Cocco.	233	*Emiliania huxleyi*	$mmol\ \#^{-1}\ h^{-1}$	Parabolic	Negative	0.0000	0.1600	0.0000
Casareto et al. (2009)	Cocco.	14	*Pleurochrysis carterae*	$mmol\ m^{-3}\ h^{-1}$	Neutral	Neutral			
White et al. (2018)	Cocco.	118	*Pleurochrysis carterae*	$mmol\ \#^{-1}$	Neutral	Neutral			
Meyer et al. (2016)	Coral	24	*Acropora millepora*	$mmol\ m^{-2}\ h^{-1}$	Neutral	Neutral			
Camp et al. (2017), Comeau et al. (2013)	Coral	74	*Acropora pulchra*	$mmol\ m^{-2}\ h^{-1}$	Parabolic	Negative	0.0000	0.2900	1.3257
Agostini et al. (2021)	Coral	18	*Acropora solitaryensis*	$mmol\ m^{-2}\ h^{-1}$	Neutral	Neutral			
Comeau et al. (2018), Comeau et al. (2019)	Coral	81	*Acropora yongei*	$mmol\ m^{-2}\ h^{-1}$	Linear +	Positive	0.0000	0.2900	1.9447
Bove et al. (2020)	Coral	27	*Duncanopsammia axifuga*	$mmol\ m^{-2}\ h^{-1}$	Linear +	Positive	0.0016	0.3300	5.0785
Cornwall et al. (2018)	Coral	44	*Goniopora* sp.	$mmol\ m^{-2}\ h^{-1}$	Neutral	Neutral			
Maier et al. (2009)	Coral	237	*Lophelia pertusa*	$mmol\ g^{-1}\ h^{-1}$	Linear +	Positive	0.0030	0.0400	0.0002
Bove et al. (2020)	Coral	65	*Montastraea cavernosa*	$mmol\ m^{-2}\ h^{-1}$	Linear +	Positive	0.0154	0.0900	0.5047
Ries et al. (2009)	Coral	54	*Oculina arbuscula*	$mmol\ g^{-1}h^{-1}$	Parabolic	Negative	0.0000	0.8600	0.0001
Comeau et al. (2013)	Coral	72	*Pavona cactus*	$mmol\ m^{-2}\ h^{-1}$	Parabolic	Negative	0.0002	0.2200	0.9093
Comeau et al. (2019)	Coral	49	*Plesiastrea versipora*	$mmol\ m^{-2}\ h^{-1}$	Linear +	Positive	0.0069	0.1500	0.6003
Brown et al. (2022)	Coral	4	*Pocillopora damicornis*	$mmol\ g^{-1}\ h^{-1}$	Neutral	Neutral			
Comeau et al. (2013, 2018), Putnam and Gates (2015)	Coral	117	*Pocillopora damicornis*	$mmol\ m^{-2}\ h^{-1}$	Neutral	Neutral			
Evensen and Edmunds (2016)	Coral	60	*Pocillopora verrucosa*	$mmol\ m^{-2}\ h^{-1}$	Linear +	Positive	0.0132	0.1000	0.8297
Agostini et al. (2021)	Coral	18	*Porites heronensis*	$mmol\ m^{-2}\ h^{-1}$	Neutral	Neutral			

Studies*	n	Group	Species	Rate unit	Response	Pos/Neg/Neut	p value	R^2	RMSE
Comeau et al. (2013)	72	Coral	*Porites rus*	$mmol\ m^{-2}\ h^{-1}$	Linear +	Positive	0.0020	0.1300	2.0281
Okazaki et al. (2013)	75	Coral	*Siderastrea radians*	$mmol\ m^{-2}\ h^{-1}$	Linear +	Positive	0.0004	0.1600	2.7886
Okazaki et al. (2013)	64	Coral	*Solenastrea hyades*	$mmol\ m^{-2}\ h^{-1}$	Threshold +	Positive	0.0004	0.2300	2.0385
Krueger et al. (2017)	36	Coral	*Stylophora pistillata*	$mmol\ m^{-2}\ h^{-1}$	Neutral	Neutral			
Pansch et al. (2014)	36	Crust.	*Amphibalanus improvisus*	$mmol\ g^{-1}\ h^{-1}$	Linear +	Positive	0.0000	0.4300	0.0004
Ries et al. (2009)	36	Crust.	*Callinectes sapidus*	$mmol\ g^{-1}\ h^{-1}$	Linear −	Negative	0.0000	0.4000	0.0082
Ries et al. (2009)	18	Crust.	*Homarus americanus*	$mmol\ g^{-1}\ h^{-1}$	Linear −	Negative	0.0014	0.4800	0.0079
Ries et al. (2009)	12	Crust.	*Penaeus plebejus*	$mmol\ g^{-1}\ h^{-1}$	Linear −	Negative	0.0124	0.4800	0.0006
Findlay et al. (2010)	6	Crust.	*Semibalanus balanoides*	$mmol\ g^{-1}\ h^{-1}$	Neutral	Neutral			
Tatters et al. (2013)	45	Dino.	*Alexandrium sp.*	$l\ h^{-1}$	Neutral	Neutral			
Hansen et al. (2007)	19	Dino.	*Ceratium lineatum*	$l\ h^{-1}$	Linear −	Negative	0.0000	0.6700	0.0043
Hansen et al. (2007)	45	Dino.	*Gonyaulax sp.*	$l\ h^{-1}$	Neutral	Neutral			
Tatters et al. (2013)	31	Dino.	*Heterocapsa triquetra*	$\#\,h^{-1}$	Threshold −	Negative	0.0000	0.9100	0.0027
Hansen et al. (2007)	4	Dino.	*Karenia mikimotoi*	$l\ h^{-1}$	Neutral	Neutral			
Wang et al. (2019)	45	Dino.	*Lingulodinium polyedrum*	$l\ h^{-1}$	Neutral	Neutral			
Tatters et al. (2013)	45	Dino.	*Prorocentrum micans*	$l\ h^{-1}$	Neutral	Neutral			
Tatters et al. (2013)	21	Dino.	*Prorocentrum minimum*	$\#\,h^{-1}$	Neutral	Neutral			
Hansen et al. (2007)	175	Dino.	*Symbiodinium sp.*	$\#\,h^{-1}$	Threshold −	Negative	0.0000	0.8800	0.0019
Brading et al. (2011)	12	Dino.	*Thoracosphaera heimii*	$mmol\ h^{-1}$	Linear −	Negative	0.0010	0.0600	0.0066
Van de Waal et al. (2013)	17	Echino.	*Arbacia punctulata*	$mmol\ h^{-1}$	Parabolic	Negative	0.0002	0.8500	0.0000
Ries et al. (2009)	4	Echino.	*Echinometra viridis*	$\%\ h^{-1}$	Linear +	Positive	0.0244	0.9500	2.3854
Courtney et al. (2013)	28	Echino.	*Echinometra viridis*	$\%$	Linear +	Positive	0.0009	0.3500	13.0388
Courtney and Ries (2015)	18	Echino.	*Eucidaris tribuloides*	$mmol\ g^{-1}\ h^{-1}$	Threshold +	Positive	0.0000	0.8400	0.0004
Ries et al. (2009)	205	Foram.	*Ammonia sp.*	$mmol\ \#^{-1}\ h^{-1}$	Linear −	Negative	0.0000	0.0200	0.0000
Keul et al. (2013)	32	Foram.	*Amphistegina lessonii*	$\%\ h^{-1}$	Parabolic	Negative	0.0277	0.3900	0.0008
Prazeres et al. (2015)	16	Foram.	*Globigerinella siphonifera*	$mmol\ h^{-1}$	Neutral	Neutral			
Kisakürek et al. (2011)	14	Foram.	*Globigerinoides ruber*	$mmol\ \#^{-1}\ h^{-1}$	Neutral	Neutral			
Kisakürek et al. (2011)	179	Foram.	*Marginopora rossi*	$mmol\ \#^{-1}\ h^{-1}$	Linear +	Positive	0.0000	0.1900	0.0090
Reymond et al. (2013)	47	Foram.	*Marginopora vertebralis*	$mmol\ g^{-1}\ h^{-1}$	Linear +	Positive	0.0000	0.4000	0.0004
Uthicke and Fabricius et al. (2012)	16	Foram.	*Marginopora vertebralis*	$mmol\ \#^{-1}\ h^{-1}$	Threshold +	Positive	0.0000	0.3300	0.0005
Sinutok et al. (2011)	32	Foram.	*Marginopora vertebralis*	$mmol\ h^{-1}$	Neutral	Neutral			
Manno et al. (2012)	192	Foram.	*Neogloboquadrina pachyderma*	$\%\ h^{-1}$	Linear −	Negative	0.0006	0.7100	0.0000
Oron et al. (2020)	96	Foram.	*Operculina ammonoides*	$mmol\ \#^{-1}\ h^{-1}$	Linear +	Positive	0.0000	0.0900	0.0017
Manríquez et al. (2016)	74	Gastropod	*Concholepas concholepas*	$mmol\ g^{-1}\ h^{-1}$	Parabolic	Negative	0.0000	0.2400	0.0009
Noisette et al. (2016), Ries et al. (2009)	173	Gastropod	*Crepidula fornicata*	$mmol\ g^{-1}\ h^{-1}$	Linear +	Positive	0.0000	0.0900	0.0028
Garilli et al. (2015)	68	Gastropod	*Cyclope neritea*	$mmol\ g^{-1}\ h^{-1}$	Linear −	Negative	0.0000	0.2100	0.0037
Ries et al. (2009)	42	Gastropod	*Littorina littorea*	$mmol\ g^{-1}\ h^{-1}$	Linear −	Negative	0.0020	0.1400	0.0002
Garilli et al. (2015)	68	Gastropod	*Littorina littorea*	$mmol\ g^{-1}\ h^{-1}$	Linear −	Negative	0.0001	0.3400	0.0064
Bibby et al. (2007)	4	Gastropod	*Littorina littorea*	µm (shell thickness)	Neutral	Neutral			
Garilli et al. (2015)	315	Gastropod	*Nassarius corniculus*	$mmol\ g^{-1}\ h^{-1}$	Parabolic	Negative	0.0000	0.2500	0.0001
Garilli et al. (2015)	21	Gastropod	*Strombus alatus*	$mmol\ g^{-1}\ h^{-1}$	Linear +	Positive	0.0000	0.6400	0.0001
Ries et al. (2009)	33	Gastropod	*Urosalpinx cinerea*	$mmol\ g^{-1}\ h^{-1}$	Linear +	Positive	0.0000	0.5700	0.0002
Ries et al. (2009)	18	Mollusks	*Argopecten irradians*	$mmol\ g^{-1}\ h^{-1}$	Linear +	Positive	0.0097	0.3500	0.0002

Studies*	n	Group	Species	Rate unit	Response	Pos/Neg/Neut	p value	R^2	RMSE
Ramajo et al. (2016)	6	Mollusks	*Argopecten purpuratus*	$\text{mmol g}^{-1}\,\text{h}^{-1}$	Neutral	Neutral			
Zhang et al. (2011)	5	Mollusks	*Azumapecten farreri*	$\text{mmol g}^{-1}\,\text{h}^{-1}$	Linear +	Positive	0.0106	0.9200	0.0001
Ong et al. (2017)	24	Mollusks	*Cerastoderma edule*	$\text{mmol g}^{-1}\,\text{h}^{-1}$	Neutral	Neutral			
Sordo et al. (2021)	27	Mollusks	*Chamelea gallina*	$\text{mmol g}^{-1}\,\text{h}^{-1}$	Neutral	Neutral			
Gazeau et al. (2007)	20	Mollusks	*Crassostrea gigas*	$\text{mmol g}^{-1}\,\text{h}^{-1}$	Linear +	Positive	0.0001	0.6100	0.0000
Ries et al. (2009), Waldbusser et al. (2011)	28	Mollusks	*Crassostrea virginica*	$\text{mmol g}^{-1}\,\text{h}^{-1}$	Threshold +	Positive	0.0000	0.5600	0.0003
Ries et al. (2009)	25	Mollusks	*Mercenaria mercenaria*	$\text{mmol g}^{-1}\,\text{h}^{-1}$	Threshold +	Positive	0.0000	0.8300	0.0000
Ries et al. (2009)	14	Mollusks	*Mya arenaria*	$\text{mmol g}^{-1}\,\text{h}^{-1}$	Linear +	Positive	0.0001	0.7300	0.0003
Ninokawa et al. (2020)	13	Mollusks	*Mytilus californianus*	$\text{mmol m}^{-2}\,\text{h}^{-1}$	Neutral	Neutral			
Ries et al. (2009), Gazeau et al. (2007)	86	Mollusks	*Mytilus edulis*	$\text{mmol g}^{-1}\,\text{h}^{-1}$	Linear +	Positive	0.0119	0.0700	0.0002
Gazeau et al. (2014)	11	Mollusks	*Mytilus galloprovincialis*	$\text{mmol g}^{-1}\,\text{h}^{-1}$	Neutral	Neutral			
Cameron et al. (2019)	30	Mollusks	*Pecten maximus*	$\text{mmol g}^{-1}\,\text{h}^{-1}$	Neutral	Neutral			
Comeau et al. (2010b)	5	Pteropod	*Cavolinia inflexa*	mm (shell length)	Neutral	Neutral			
Comeau et al. (2009, 2010a)	12	Pteropod	*Limacina helicina*	$\text{mmol g}^{-1}\,\text{h}^{-1}$	Linear +	Positive	0.0000	0.8500	0.0001
Lischka et al. (2011), Lischka and Riebesell (2012)	119	Pteropod	*Limacina helicina*	mm (shell length)	Threshold +	Positive	0.0003	0.1300	0.1303
Bednaršek (2021a), Mekkes et al. (2021)	117	Pteropod	*Limacina helicina*	μm (shell thickness)	Parabolic	Negative	0.0000	0.1800	0.0038
Lischka and Riebesell (2012)	28	Pteropod	*Limacina retroversa*	mm (shell length)	Neutral	Neutral			

* Barcelos e Ramos et al. (2010), Fiorini et al. (2011), Iglesias-Rodriguez et al. (2008), Richier et al. (2011), Sciandra et al. (2003), Stoll et al. (2012), Gafar and Schulz (2018), Bach et al. (2011), and Sett et al. (2014).

ing Ω_{ar} of 10. This indicates the potential of leveraging such experimental studies as a baseline for predictive regression models of biological responses to a range of Ω_{ar} conditions, as expected under OAE studies.

Once the biological data were compiled, units were standardized where possible. The main issue when compiling data was the lack of standardization of the calcification rates. A variety of calcification rate units were used across different studies. Where possible, the units were converted to millimoles of $CaCO_3$ g per gram per hour. However, the data required to do so were not always readily available. Other units used for calcification rate were millimoles of $CaCO_3\ \text{m}^{-2}\,\text{h}^{-1}$ and millimoles of $CaCO_3\ \text{m}^{-3}\,\text{h}^{-1}$, and there were also data used as an indication of calcification rate with units of $\text{mmol \#}^{-1}\,\text{h}^{-1}$, mmol h^{-1}, mmol cm^{-2}, and $\%\,\text{h}^{-1}$, where "#" indicates one individual. Growth rates and particulate inorganic carbon (PIC) production rates were used as indicators of calcification rate for single-cell organisms. For some species, direct calcification rates were not reported in the literature; instead only relevant parameters related to calcification (shell length, density, thickness) over time were available from the experimental studies. The decision was made to also collect these additional datasets because the statistical analyses of this study focus on the trend in absolute numbers and would not change by being transformed into the rates. Data were analyzed on a species level, wherever rate units were the same. Hereafter, this is referred to as the species rate group. Where there were multiple studies available for the calcification rate of one species using the same rate units, the data were combined (e.g., *Emiliania huxleyi*).

2.4 Sorting species-specific responses into categories per calcification response

Responses were split into six categories: linear positive and linear negative, parabolic, threshold positive and negative, and neutral. The response was determined with a best-fit regression model, using the ordinary least squares method in Statsmodels for Python (see Seabold and Perktold, 2010). See Fig. 2 for examples of these responses of calcification rate to increasing TA : DIC ratio.

The final response for each species was determined by the regression with the lowest p value. This method is in contrast with the Ries et al. (2009) study where they chose the regression analysis that yielded the lowest square root of the mean squared error (RMSE) for a given species and that was statistically significant ($p \leq 0.05$). When applying their method to our data, parabolic and exponential regressions were always favored over linear regressions. When examining these regressions, we found that choosing the best fit based on the lowest p value yielded better fits, as this method prevents overfitting due to noise in the data. Where a linear regression had the best fit, we assigned a linear response, which could be either positive or negative based on the slope. The species

with a significant exponential fit were categorized as threshold positive ($+$) or threshold negative ($-$), which was distinguished from the parabolic response with the fitted parabolic curve.

The best-fit regression was assigned to each species and plotted but only if the p value was considered significant, i.e., lower than 0.05. These regressions were plotted along with a 90 % prediction interval, which accounts for the variability of the experimental data. The species with a p value > 0.05 were categorized as having no correlation (neutral response).

When multiple datasets obtained from different studies for the same species and rate units could not be combined, we took each response into consideration and reported the p value and RMSE for each of the studies. Even when different studies reported varying calcification rates for the same species, we refrained from selecting a single overall species response; rather, we analyzed each species individually. The TA : DIC threshold was computed to indicate the point at which the current calcification rate (i.e., the calcification rate at the baseline) is reduced by a half for linear negative, threshold negative, and parabolic responders. The thresholds and the amount of NaOH and Na_2CO_3 required (starting at $10\,\mu mol\,kg^{-1}$ and then in steps of $50\,\mu mol\,kg^{-1}$) to reach this threshold were determined, dependent on local temperature and salinity conditions. For parabolic responders, the inflection points that tell us when the rate is predicted to change slope are also included in Table S2. Once the species' responses were determined, an attempt was made to group them based on functional groups. However, since species within the same functional group had varying responses, grouping them together meant these responses were no longer visible due to a wide spread of data. Therefore, most of the analysis remained at the species level (Table 1).

2.5 Conceptual framework to evaluate increases in TA : DIC

The regression models applied to each species could be used to predict calcification rates at a higher TA : DIC ratio. We conceptually added alkalinity from the current calcification rate baseline. This baseline was computed for each species using CO2SYS with $pCO_2 = 425\,ppm$ and $pH_T = 8.1$, for the average temperature and salinity for each species rate group, based on their respective OA dataset(s) (see Table S3). All CO2SYS calculations in this study were carried out with the Python version of CO2SYS (Humphreys et al., 2022) using the stoichiometric dissociation constants for carbonic acid from Sulpis et al. (2020), for sulfuric acid by Dickson (1990), and for total boron from Uppström (1974). From this baseline, TA was added in the form of both NaOH and Na_2CO_3 to approximate changes in the carbonate chemistry settings, with NaOH changing TA : DIC in the $1:1$ ratio and Na_2CO_3 inducing a $2:1$ TA : DIC change. For example, $10\,\mu mol\,kg^{-1}$ of NaOH addition will increase TA by $10\,\mu mol\,kg^{-1}$ and not affect DIC.

For Na_2CO_3, a $10\,\mu mol\,kg^{-1}$ addition will increase TA by $10\,\mu mol\,kg^{-1}$ and increase DIC by $5\,\mu mol\,kg^{-1}$. Figure 1 demonstrates the usefulness of this approach. For both NaOH and Na_2CO_3, $10\,\mu mol\,kg^{-1}$ was conceptually added using the principles of mass balance approach for the carbonate system via CO2SYS. This was repeated for increments of $50\,\mu mol\,kg^{-1}$. We show this incremental addition in the plots until a total of $500\,\mu mol\,kg^{-1}$ when generating the plots. When computing the thresholds, we added up to $1400\,\mu mol\,kg^{-1}$ NaOH. The new TA : DIC ratios were estimated by adding the direct effect of ΔTA and ΔDIC due to chemical additions of NaOH (assume $\Delta DIC = 0$) or Na_2CO_3 (assume $\Delta DIC = 0.5 \cdot \Delta TA$). A maximum of $500\,\mu mol\,kg^{-1}$ was chosen to have more realistic additions of TA that resemble those appropriate within the OAE field trials (e.g., Wang et al., 2023). With the new TA : DIC ratios after TA addition, the species' regression models based on the fitted OA response data were used to compute respective calcification rates (note that added points with NaOH or Na_2CO_3 were not calculated as part of the regression). These data points were all plotted along with the experimental data, regression model, and prediction intervals, as shown in Fig. 3.

We also determine the amount of NaOH and Na_2CO_3 needed to reach pH_T 9 for each study. This was computed for each species rate group using CO2SYS starting from $pCO_2 = 425\,ppm$ and $pH_T = 8.1$, using the average temperature and salinity per species rate group and by adding NaOH or Na_2CO_3 in increments of $50\,\mu mol\,kg^{-1}$ until pH_T 9 was reached. Note that this method does not incorporate gas exchange with the atmosphere, any biological processes, organic matter effects, nitrification and/or denitrification, complexation, speciation, or sediment–water interactions.

2.6 Evaluation of the biological responses based on alkalinity addition

The individual species with significant correlations were grouped visually based on their best-fit regression models and are classified into positive, negative, and neutral as follows:

1. *Positive responders* are species with predicted *linear positive* and *threshold positive* calcification rate response with increased TA addition.

2. *Negative responders* are species with predicted *linear negative*, *parabolic*, and *threshold negative response* in calcification rate upon (a certain amount of) TA addition. For the parabolic responders, a concentration of NaOH was determined that indicates the threshold in TA : DIC beyond which the response becomes negative (see inflection points in Table S2).

3. *Neutral responders* are species with *no significant correlation* ($p < 0.05$) in calcification rate upon TA addition.
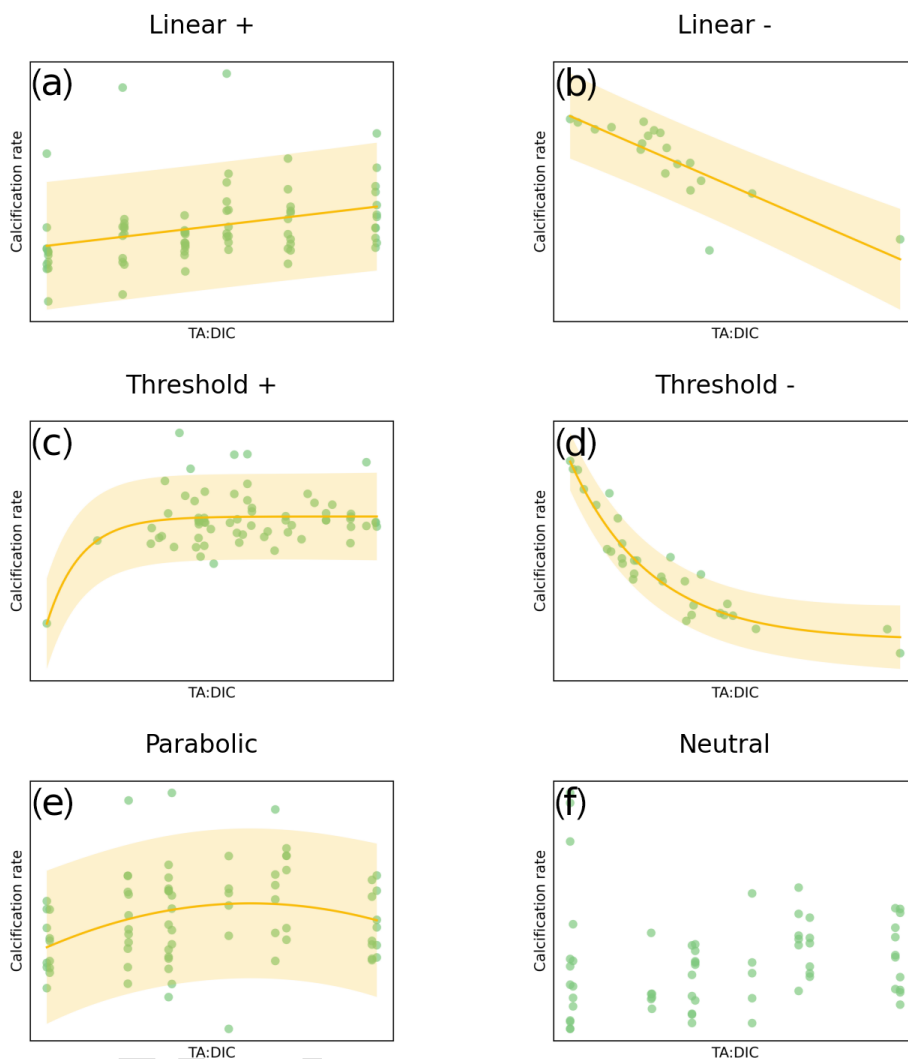
Figure 2. Examples of the categories of responses between carbonate chemistry parameters (TA : DIC) and calcification rate: **(a)** linear positive (calcification increase with increased TA : DIC); **(b)** linear negative (calcification decrease with increased TA : DIC); **(c)** exponential for the threshold positive response (calcification increase, plateauing at higher TA : DIC); **(d)** exponential for the threshold negative response (calcification decline, plateauing at lower TA : DIC); **(e)** parabolic (calcification increase followed by a decrease at higher TA : DIC); and **(f)** neutral (non-significant) response. Responses were only considered significant when $p < 0.05$; otherwise they were categorized as neutral. Yellow shading represents the 90 % prediction interval. Note that TA : DIC on the x axis corresponds to pH_T and Ω_{ar}, as these variables have an approximately linear relationship at a particular salinity, temperature, and pressure (see Fig. 1).

2.7 Determining threshold values indicative of negative biological response to OAE

The metrics to evaluate the sensitivity of calcification rate of the negative responders in this study were based on the amount of NaOH or Na_2CO_3 addition required to reduce the current calcification rate by half. The greater the TA : DIC ratio value required to trigger half the calcification rate reduction, the less sensitive the species was to NaOH addition. We refer to this TA : DIC ratio as the biological threshold, which we also report along with corresponding pH and Ω_{ar} and the associated uncertainty. TA : DIC thresholds were converted to their respective pH and Ω_{ar}, which are affected by temper-

ature and salinity. To calculate threshold pH and Ω_{ar}, we used the average temperature and salinity per species rate group, as done for calculating the baseline.

2.8 Extraction of the carbonate chemistry data from the GLODAP dataset

We extracted total alkalinity, dissolved inorganic carbon, Ω_{ar}, and pH_T from the Global Ocean Data Analysis Project GLODAPv2.2023 dataset (https://glodap.info, last access: 6 April 2024). We used the regression application in MAT-LAB with a second-order polynomial equation to predict Ω_{ar} from TA : DIC. The regression analysis was performed

using data from various depth intervals (0–10, 0–30, 0–50, 0–100, 0–200 m) regionally and globally. The regional analysis divided the global oceans into the following groupings: Arctic (north of 65° N), Southern Ocean (south of 40° S), North Pacific (north of 40° N), Central Pacific (40° S to 40° N), North Atlantic (North of 40° N), Central Atlantic (40° S to 40° N), and Indian Ocean (north of 40° S).

3 Results

3.1 Data collection for the calcification rate responses of different biological groups

We examined 68 datasets, which covered 84 different species that were divided into 11 different groups (Fig. 4). These functional groups were corals (20 % of datasets), calcifying algae (18 %), mollusks (14 %), foraminifera (10 %), dinoflagellates (10 %), coccolithophores (4 %), gastropods (8 %), crustaceans (5 %), echinoderms (4 %), pteropods (5 %), and annelids (1 %). In the mollusk group, we have separated out gastropods and pteropods because of a higher number of studies that explicitly cover these two groups. The group of gastropods refers to all gastropods that are not pteropods. If all three groups were combined (mollusks, gastropods, pteropods), this group would be the largest.

3.2 Species-specific responses to NaOH / Na$_2$CO$_3$ addition

Calcification rate responses of species from different groups were correlated to TA : DIC and summarized to obtain calcification rate response. The calcification rate responses encompassed linear (positive and negative), threshold (positive and negative), parabolic, and neutral responses, with the slope and the intercept of the response determining the type and the magnitude of the response. We present fitted responses of calcification rate per TA : DIC ratio for each examined species (Table 1; Fig. S4). When possible, we fit a regression to multiple datasets of the same species that used the same calcification units. We also present the response with the additions of NaOH and Na$_2$CO$_3$ for each species per examined study and corresponding rate unit and their biological TA : DIC thresholds (Tables 2, S4).

Within each of the 11 functional groups, several categories of calcification response occur within each functional group, with the most varied being the group of dinoflagellates and foraminifera, both showing 4 or 5 different categories of calcification responses (Fig. 5). Of the six types of responses of calcification rate vs. TA : DIC, 28 % were linear positive ($N = 27$), 9 % linear negative ($N = 9$), 6 % threshold positive ($N = 6$), 2 % threshold negative ($N = 2$), 15 % parabolic ($N = 14$), and 40 % neutral ($N = 38$).

Such responses could be further summed up into positive (linear and threshold positive), negative (linear and threshold negative, parabolic), and neutral responses (Fig. 6) when

generalized for calcification rate against the TA : DIC ratio. A summary of responses includes 34.4 % positive ($N = 33$) and 26.0 % negative ($N = 25$), while 39.6 % of responses show a neutral response ($N = 38$).

3.3 Evaluation of the responses to NaOH / Na$_2$CO$_3$ addition

Upon added TA, the calcification rate in positive responders will increase, either in a linear or threshold positive response, where calcification plateaus, with the concentration being dependent on the species-specific rate of response (Figs. 2, S4). The negative responders (linear or threshold negative and parabolic) will be negatively impacted as follows: first, for the linear negative responders, addition of the Na$_2$CO$_3$ will linearly decrease calcification rate, but there is no associated threshold to it; second, for the threshold negative responders, calcification rate will decline in an exponential way until reaching a TA : DIC value where the response plateaus; and, third, for the parabolic responders, the calcification rate will initially increase until reaching a certain TA : DIC threshold upon which calcification starts declining. The TA : DIC thresholds for negative responders are species-specific (Tables 2, S4).

3.4 Threshold values indicative of negative biological response to OAE

The TA : DIC biological thresholds in Table 2 are determined by the amount of NaOH addition required to reduce calcification rate by half (see Table S4 for Na$_2$CO$_3$ thresholds). These thresholds demonstrate the range of carbonate chemistry conditions over which the negative biological effects of OAE deployment might occur over the short term in the near-field and are shown alongside the corresponding pH$_T$ and Ω_{ar}. Uncertainties are higher for the experimental studies where the experimental temperature and salinity ranges were high (see Table S5), seeing as we use the average for each species rate group to compute the baseline and thresholds.

For the negative responders, TA : DIC thresholds range from 1.13 to 1.74. The majority of species have reached their thresholds by an addition of 500 μmol kg^{-1} NaOH, though for three species a NaOH addition of more than 500 μmol kg^{-1} is required to cross the thresholds in the TA : DIC range of 1.39 to 1.74. *Crepidula fornicata* (gastropod), *Neogoniolithon* sp. (algae), *Homarus americanus* (crustacean), and *Oculina arbuscula* (coral) reach their thresholds by 100 μmol kg^{-1} addition of NaOH, indicating they are more sensitive to alkalinity addition. Foraminifera, dinoflagellates, and coccolithophores generally require higher concentrations of NaOH to reach their thresholds, with the linear negative responder *Ammonia* sp. of the foraminifera group requiring 1400 μmol kg^{-1} to reduce calcification rate in half.
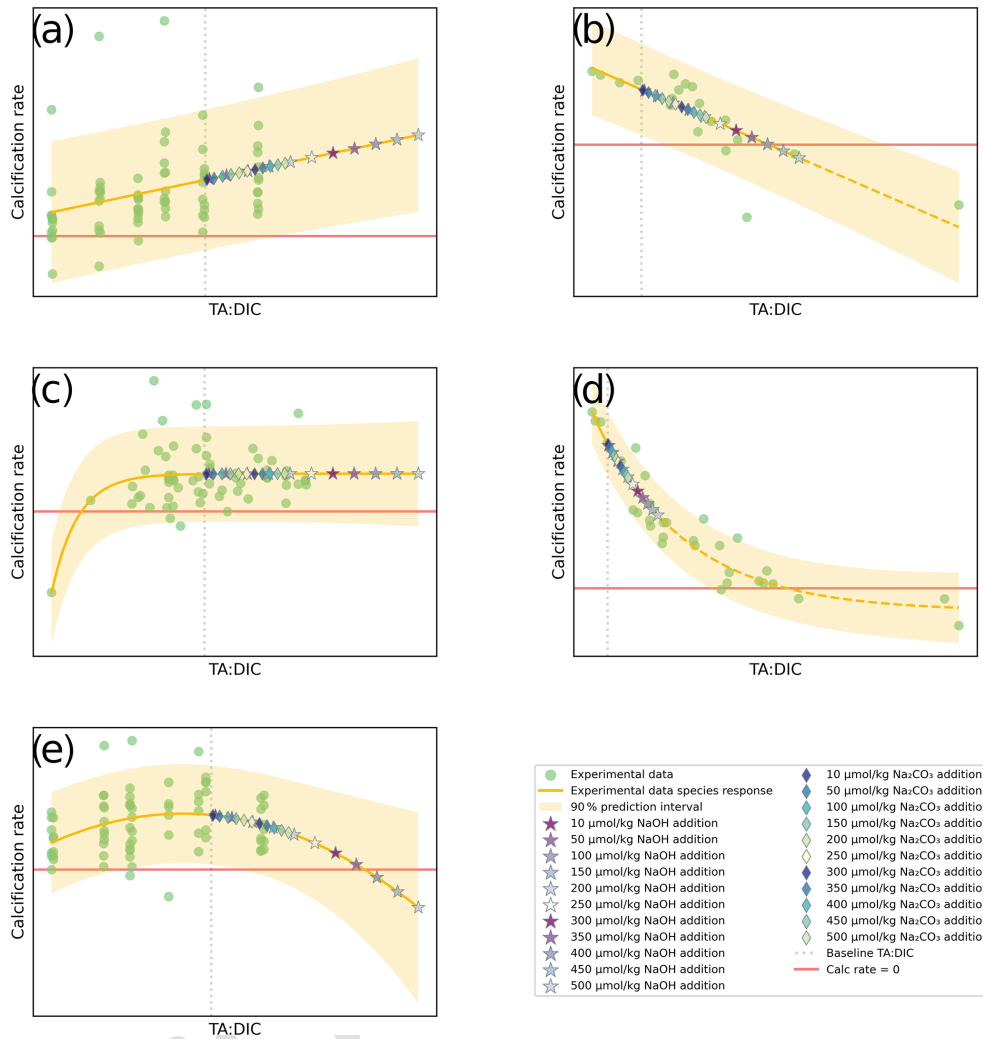
Figure 3. Conceptual diagrams for five types of responses: **(a)** linear positive, **(b)** linear negative, **(c)** threshold positive, **(d)** threshold negative, and **(e)** parabolic response, plotted with experimental data from OA studies (green dots), predicted values at various additions of alkalinity (stars and diamonds), the regression line, and prediction error margins fitted for a given species. The red horizontal line indicates zero net dissolution (calcification rate is equal to 0; dissolution rate = calcification rate). The gray vertical line indicates the baseline to which alkalinity is added. NaOH and Na_2CO_3 addition is shown up to $500 \, \mu mol \, kg^{-1}$.

For some negative responders (*Arbacia punctulata, Nassarius corniculus, Penaeus plebejus, Callinectes sapidus, Cyclope neritea*, and *Symbiodinium* sp.), the baseline from which NaOH addition occurs was outside of the range of the experimental data and very close to a calcification rate of 0. These were omitted from Table 2 since our defined threshold does not give an accurate representation of their sensitivity to alkalinity addition. *Limacina helicina* was also omitted since the indicator of calcification (shell thickness) was not an actual rate.

3.5 Regulatory pH$_T$ 9 threshold

We also compute how much NaOH and Na_2CO_3 need to be added before reaching a pH$_T$ threshold of 9, as per the US Environmental Protection Agency's rule for wastewater not exceeding a pH$_T$ of 9 when entering the coastal ocean (NPDES manual, 2010). This amount averages $1200 \, \mu mol \, kg^{-1}$ of NaOH and $4700 \, \mu mol \, kg^{-1}$ of Na_2CO_3 for most of the examined species. For some species (*Amphibalanus improvisus*, *Neogloboquadrina pachyderma*, *Limacina helicina*, *Limacina retroversa*, *Lophelia pertusa* , and *Semibalanus balanoides*), their threshold was reached below $1000 \, \mu mol \, kg^{-1}$ NaOH and $3000 \, \mu mol \, kg^{-1}$ Na_2CO_3, with *Amphibalanus improvisus* reaching a threshold at $750 \, \mu mol \, kg^{-1}$ NaOH and $2250 \, \mu mol \, kg^{-1}$ Na_2CO_3.

Table 2. Studies with negative responders (linear and threshold negative, parabolic) with demonstrated negative calcification rate (i.e., at the baseline). The value for TA : DIC threshold is used to determine the pH_T and Ω_{ar} (at average temperature and average salinity per species). See Table S4 for Na_2CO_3 thresholds.

Studies	Group	Species	Temperature (°C)	Salinity	Rate unit	Threshold	TA addition	pH_T at threshold	ΔpH_T from baseline	Ω_{ar} at threshold	Exposure time
Noisette et al. (2016), Ries et al. (2009)	Gastro.	*Crepidula fornicata*	15.31	34.33	$mmol\,g^{-1}\,h^{-1}$	1.13	50	8.17	0.07	3.77	6 months, 60 d
Ries et al. (2009)	Algae	*Neogoniolithon* sp.	25.00	31.70	$mmol\,g^{-1}\,h^{-1}$	1.17	50	8.16	0.06	4.87	60 d
Ries et al. (2009)	Crust.	*Homarus americanus*	25.02	31.96	$mmol\,g^{-1}\,h^{-1}$	1.19	100	8.22	0.12	5.49	60 d
Ries et al. (2009)	Coral	*Oculina arbuscula*	25.01	31.61	$mmol\,g^{-1}\,h^{-1}$	1.19	100	8.22	0.12	5.46	60 d
Prazeres et al. (2015)	Foram.	*Amphistegina lessonii*	24.18	33.46	$\%\,h^{-1}$	1.21	150	8.27	0.17	6.10	30 d
Hansen et al. (2007)	Dino.	*Ceratium lineatum*	15.00	30.00	$\#\,h^{-1}$	1.18	200	8.38	0.28	5.15	14 d acclimation; 7 d; 14 d exposure; 22 d stationary growth phase
Sinutok et al. (2011)	Algae	*Halimeda macroloba*	27.23	36.27	$mmol\,g^{-1}\,h^{-1}$	1.26	200	8.30	0.20	7.38	2-week acclimation, 2-week incubation
Comeau et al. (2019)	Algae	*Sporolithon durum*	20.60	35.87	$mmol\,m^{-2}\,h^{-1}$	1.22	200	8.32	0.22	6.31	27 weeks
Van de Waal et al. (2013)	Dino.	*Thoracosphaera heimii*	15.00	34.00	$mmol\,h^{-1}$	1.23	300	8.46	0.36	6.56	21 d acclimation, 8 d experiment = total of > 10 generations
Camp et al. (2017), Comeau et al. (2013)	Coral	*Acropora pulchra*	27.30	36.27	$mmol\,m^{-2}\,h^{-1}$	1.38	500	8.52	0.42	11.05	N7A (natural conditions) 2-week acclimation; 2-week incubation
Hansen et al. (2007)	Dino.	*Heterocapsa triquetra*	15.00	30.00	$\#\,h^{-1}$	1.30	500	8.66	0.56	8.81	14 d acclimation; 7 d acclimation to experimental conditions; 14 d exposure; 22 d stationary growth phase
Oron et al. (2020)	Foram.	*Operculina ammonoides*	25.00	37.00	$mmol\,g^{-1}\,h^{-1}$	1.33	400	8.46	0.36	9.44	65–120 h
Prazeres et al. (2015)	Foram.	*Marginopora vertebralis*	24.18	33.46	$\%\,h^{-1}$	1.33	450	8.53	0.43	9.78	30 d
Comeau et al. (2013)	Coral	*Pavona cactus*	27.23	36.28	$mmol\,m^{-2}\,h^{-1}$	1.38	500	8.52	0.42	11.03	2-week acclimation; 2-week incubation
Hansen et al. (2007)	Dino.	*Prorocentrum minimum*	15.00	30.00	$\#\,h^{-1}$	1.39	700	8.81	0.71	11.35	14 d acclimation; 7 d acclimation to experimental conditions; 14 d exposure; 22 d stationary growth phase
Barcelos e Ramos et al. (2010), Fiorini et al. (2011), Iglesias-Rodríguez et al. (2008), Richier et al. (2011), Sciandra et al. (2003), Stoll et al. (2012), Gafar and Schulz (2018), Bach et al. (2011), and Sett et al. (2014).	Cocco.	*Emiliania huxleyi*	17.30	35.12	$mmol\,\#^{-1}\,h^{-1}$	1.46	850	8.83	0.73	13.65	26 h, acclimation for 7 generations, experiment/sampling for 2–3 generations, n/a: not applicable, 8 d, 16 d, acclimation for 12 generations, pre-acclimation for 8–12 generations, 9 generations, acclimated for at ∼ 7 generations, acclimated for at ∼ 7 generations (5–15 d).
Keul et al. (2013)	Foram.	*Ammonia* sp.	26.00	32.75	$mmol\,\#^{-1}\,h^{-1}$	1.74	1400	9.11	1.01	22.27	59–96 d of culturing
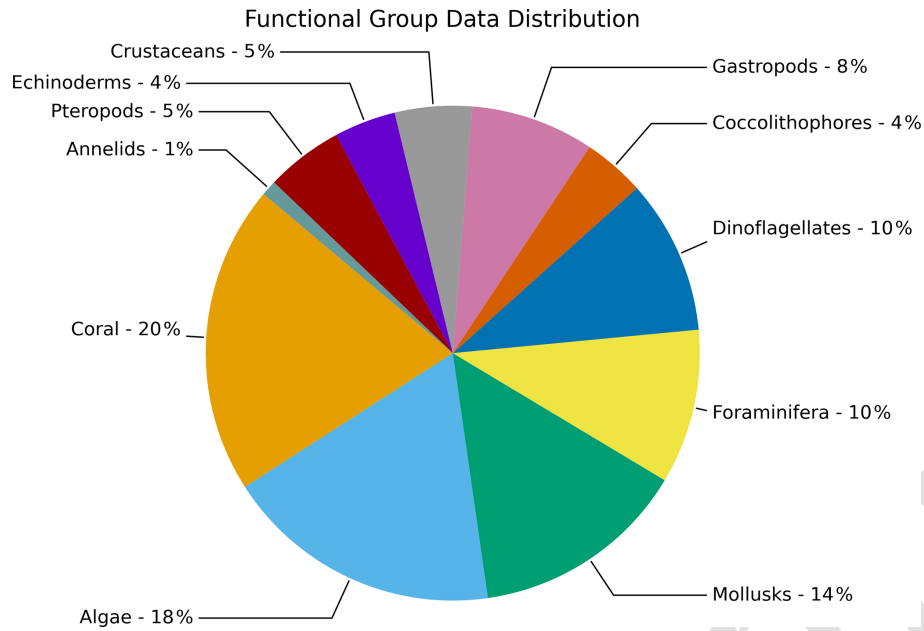
Figure 4. Percent of studies for multiple groups ($N = 11$) with available data for the calcification rate responses as part of data compilation of 68 studies covering 84 species.
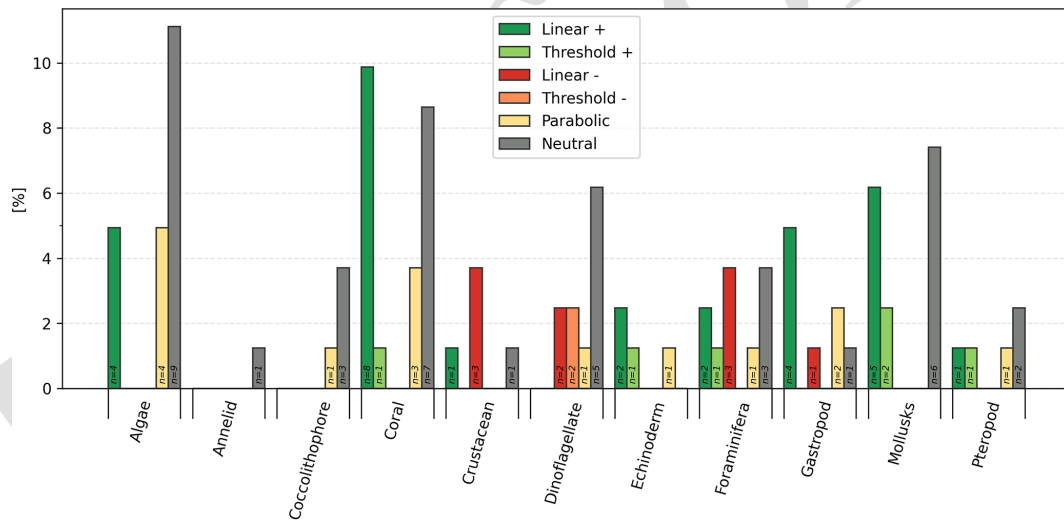
Figure 5. Categories of calcification rate responses and percentage (%) response across 11 groups (calcifying algae, annelids, coccolithophores, corals, crustaceans, dinoflagellate, echinoderms, foraminifera, gastropods, mollusks, pteropods). The number on the bar indicates the number of studies of species included.

3.6 Global and regional carbonate chemistry data coverage based on GLODAP datasets

The compilation of chemical observational data (pH, Ω_{ar}, TA, DIC) was done for the GLODAP data across the regional ocean and global scales to determine the range of Ω_{ar}, TA, and DIC (as represented by the TA : DIC ratio) and TA : DIC vs. Ω_{ar} correlation down to the depths averaged over 200 m. This allowed us to apply the thresholds even for the regions for which we do not have sufficient or reliable data or experimental coverage, making the inferences about the OAE impact even in those regions.

Here, we focused on showing the results ranging over 0–50 m because this covers most of the biological habitat for examined species, and it is where the OAE enhancement would induce the greatest changes. Over 0–50 m depth, Ω_{ar} ranges from 0.2 to 5, and TA : DIC ranges from 0.1 to 1.25. Both parameters are correlated across all regions, as demonstrated by the fitted second-order polynomial regressions, with R^2
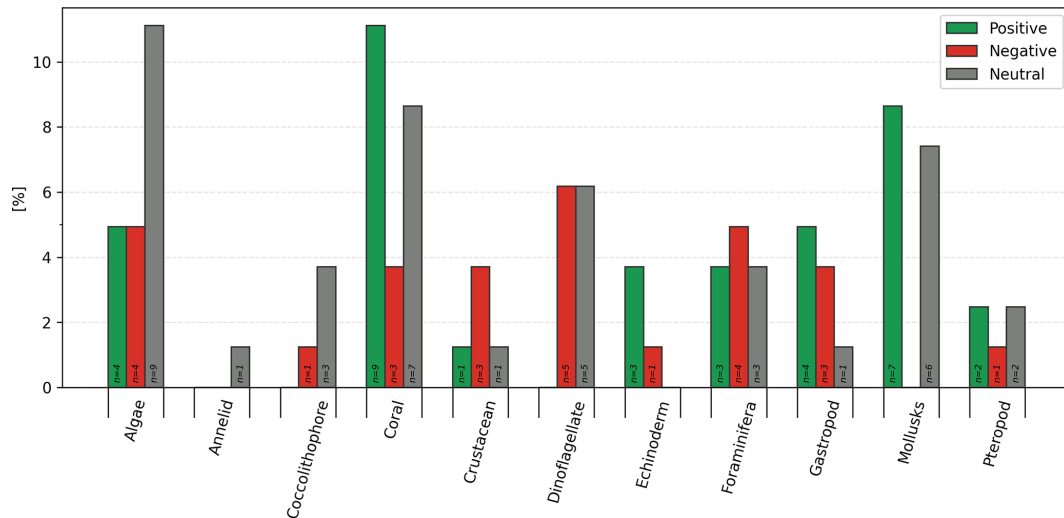
Figure 6. Summary of percentage (%) responses in calcification rates as positive (linear and threshold positive), negative (linear and threshold negative, parabolic), and neutral across 11 groups (calcifying algae, annelids, coccolithophores, corals, crustaceans, dinoflagellate, echinoderms, foraminifera, gastropods, mollusks, pteropods). The number on the bar indicates the number of studies with species included.

of 0.96 or higher, and all correlations are significant (Fig. 7), with regional specific relationships not impacting the fit. All correlation parameters are presented in Table S4. Similar fits were found at different depths. The conditions in the higher-latitude regions are located in the lower range of Ω_{ar} vs. TA : DIC, while the conditions in the low latitudes and temperate regions are in the upper range, with the highest values present in the Central Atlantic and Pacific regions. Such a strong correlation as observed for Ω_{ar} vs. TA : DIC does not exist with pH, regardless of the depth interval examined. While the correlations are still significant, they are broadly distributed and represented over a shorter TA : DIC range, with a significantly lower goodness of fit (Fig. S4), with the correlations being highly regionally dependent due to pH and temperature colinearity. Because of this, all further biological analyses are only done using the Ω_{ar} vs. TA : DIC ratio.

3.7 TA : DIC vs. Ω_{ar} for experimental data and GLODAP

We compared the ranges of TA : DIC and Ω_{ar} of biological experimental data with field biogeochemical data (GLODAP) to examine whether similar ranges of conditions and TA : DIC correlations are applicable over a broader, global dataset. For this, we plotted Ω_{ar} vs. TA : DIC along with the GLODAP regression line for Ω_{ar} vs. TA : DIC (Fig. 8). For each TA and DIC data point, the corresponding salinity-specific and temperature-specific values for that data point were used to compute Ω_{ar}. We show the similarity in the conditions, which gives the validity of our experimentally derived thresholds to be extrapolated within the global GLODAP dataset.

Figure 8 also shows that various biological groups are clustered around specific TA : DIC ratios. For example, mollusks, corals, and coccolithophores are represented on the lower, middle, and higher TA : DIC spectra, respectively, while dinoflagellates are randomly scattered off the TA : DIC line. This indicates that there is a general lack of data distribution in the upper ranges of TA : DIC ratio, especially for the groups that are lying at the lower and middle end of the TA : DIC ratio spectra. Plotting biological data from the OA datasets against the regional and global TA : DIC gradient derived from GLODAP (Fig. 7), we also observed that experimental data ranges were not always consistent with natural conditions, for example, having a lower Ω_{ar} at a higher TA : DIC ratio.

4 Discussion

OAE is a quickly developing strategy that is in the field-testing phase despite extremely limited understanding of the sequestration potential, biological implications, and environmental concerns. Hence, gaining insights into the potential risks for the biological species and communities is essential and timely. In retrospect, it took decades for the OA research community to get a more accurate and comprehensive understanding, leading to predictions of biological responses to OA (Riebesell and Gattuso, 2015). Without a very clear conceptual strategy for OAE testing, the research community might also need years to decades before OAE-related implications are comprehensively understood. Consequently, there is an essential need to develop an assessment framework of predictive responses and testing strategies that will assist in OAE scaling and risk avoidance. This paper aims at develop-
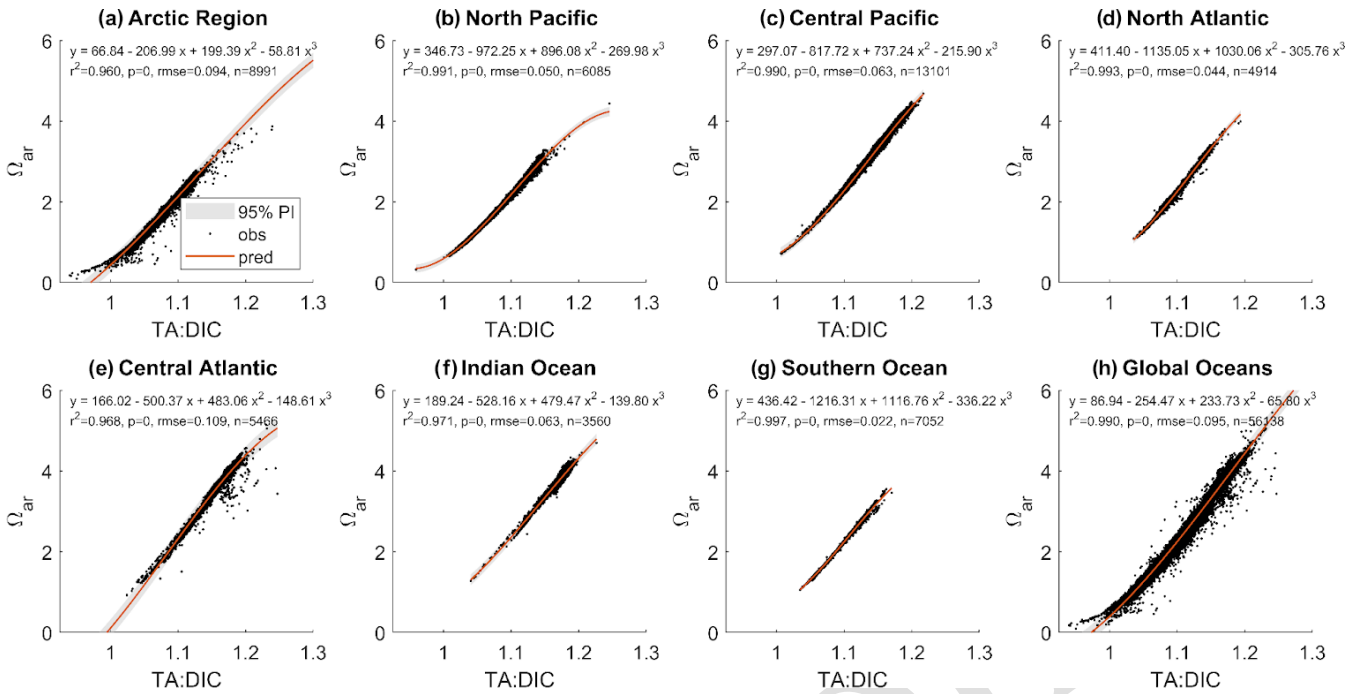
Figure 7. The range of observed Ω_{ar}, TA, and DIC values (as represented by the TA : DIC ratio) and the relationship with the best fitted curve between Ω_{ar} vs. TA : DIC across regional **(a–g)** and global **(h)** scales based on the observational GLODAP dataset averaged over the 0–50 m depth range.
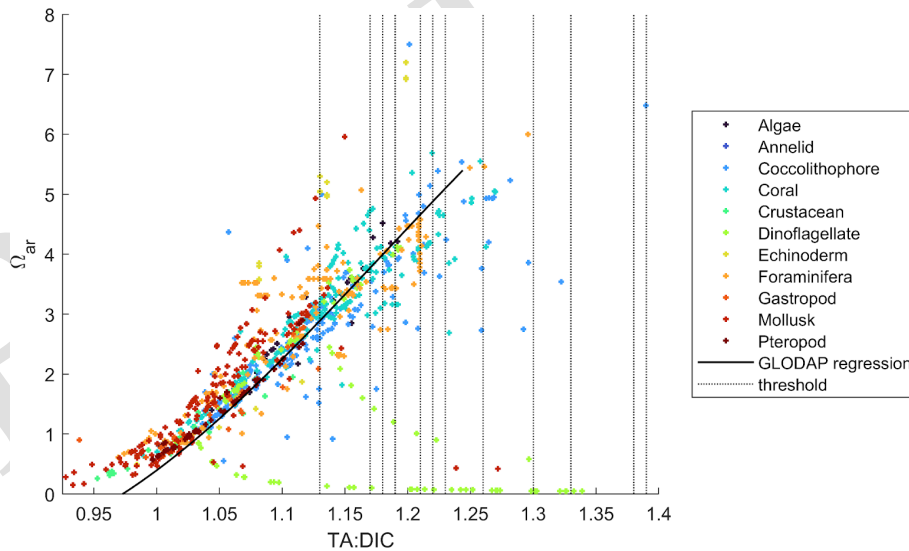
Figure 8. Ω_{ar} values from experimental biological studies for 11 investigated functional groups (see legend) plotted against TA : DIC, with the latter being computed using experimental TA and DIC. The black line represents the regression line of TA : DIC and Ω_{ar} data from the GLODAP dataset (covering 0–50 m depth). See Fig. S5 for GLODAP Ω_{ar} vs. TA : DIC, from which the black regression line shown here is derived. The vertical dotted lines represent the thresholds shown in Table 2.

ing such an assessment, where calcification responses against TA : DIC are categorized per species. We propose to use the TA : DIC ratio in biological studies reporting OAE results, as we believe it simplifies the system and makes it easier to use and translate the carbonate chemistry in the experimental set-

ting. Such a TA : DIC ratio allows us to ultimately standard-ize the biogeochemical and biological data and is useful for easier comparisons among the conducted experiments. CE8

4.1 Identified strengths and limitations of the synthesis approach based on OA studies

Prior to conducting this study, several drawbacks were identified that could potentially limit such a synthesis work: first, an insufficient amount of data at the upper range of carbonate chemistry conditions (high pH, high Ω_{ar}); second, experimental data under conditions with no relevance to natural settings (Fig. 8); and, third, an insufficient number of validation studies under high TA conditions to validate the results of this synthesis. To overcome the first two limitations, the decision was made to combine multiple OA datasets for a single species with the aim of achieving a greater range in carbonate chemistry conditions, including higher pH and Ω_{ar} experimental values, which should reduce the uncertainty of the predictions. However, combining raw data on species calcification rate proved to be more challenging because even across the same species the reporting of the calcification rates was highly variable. The use of different measuring approaches of calcification rates while conducting OA studies generated data with divergent units that do not allow for the intercomparison of data and results. As different studies for a single species could not be combined, we chose to increase the number of studies and, thus, the number of examined species. Based on the response categories from the OA studies (Ries et al., 2009), our hypothesis was that OAE will elucidate the same categories of responses, i.e., positive, negative, and neutral. Within each of the groups examined, multiple categories of predicted calcification response were found. In this way, we demonstrated that it was possible to develop a useful framework for assessing and predicting species-specific OAE responses that can delineate different responders, identify species with greater OAE sensitivity, and determine the thresholds where such negative responses could happen.

4.2 Synthesizing biological response under OAE identifies positive and negative responders

The responses were summarized across three emerging groups of responses: positive, negative, and neutral (Fig. 6). We observe species-specific variability at the species level, which is related to various calcification mechanisms across the observed groups. The greatest variability upon NaOH addition within each group in calcification rate was evident in corals, dinoflagellates, foraminifera, gastropods, and pteropods, where four to five different categories of responses were found.

Positive responders (34 %) show an increased calcification rate upon alkalinity addition, observed within all functional groups besides annelids, coccolithophores, and dinoflagellates. Corals mostly have positive and neutral responses, suggesting that coral species would not be negatively impacted during OAE field trials. This mostly positive response is validated by increased coral calcification, shown for two coral species of *Acropora* and *Siderastrea* in experiments conducted by Palmer (2022).

The metrics to evaluate the sensitivity of calcification rate for the negative responders (negative linear and threshold) to alkalinity addition were based on the amount of alkalinity addition required to halve the current calcification rate (Fig. 3; Tables 1, 2). The most negative responses were found in dinoflagellates (6 % of all species), algae, and foraminifera (both 5 % of all species). However, these numbers are affected by the difference in data coverage per functional group. When comparing the ratio of negative to positive and neutral responses, crustaceans and dinoflagellates are expected to be most negatively affected. As such, these groups are one of the priorities for the future OAE experimental work to determine at which TA : DIC negative response happens. Dinoflagellates demonstrate negative response in five cases, five neutral responses, and zero positive (see Table 1; Fig. S4). The reason for negative response to OAE in this group is related to the fact that their growth gets limited at a higher pH, with further carbon limitation playing a role at very high pH levels and low DIC concentration (Hansen et al., 2007; Hansen, 2002). On the other hand, crustaceans only demonstrated positive response in one study (Pansch et al., 2014), while remaining results predict either a negative or neutral response. While crustaceans are effective in retaining homeostasis at lower pH, they might be less so at higher pH, which was shown in the OA experiments by Ries et al. (2009) for three crustacean species (*Callinectes sapidus, Homarus americanus, Penaeus plebejus*), confirmed in the OAE study by Cripps et al. (2013) in *Carcinus maenas*. While studies are still lacking, physiological acid–base regulation at higher pH is associated with higher costs (Cripps et al., 2013). Crustaceans show a disrupted acid–base balance, evident through the increase in hemolymph pH, K^+, Na^+ ions, and osmolality, coupled with a decrease in extracellular $p\mathrm{CO}_2$ and HCO_3^-, indicative of respiratory alkalosis (Truchot, 1984, 1986). This is often associated with hyperventilation, the aim of which is to flush out the hemolymph CO_2 to increase the affinity of oxygen uptake. However, while this might be a temporary physiological relief, it also implies energetic costs, potentially also for calcification.

For the neutral responders or groups with no significant correlation between calcification rates and TA : DIC, it is somewhat uncertain to predict whether such responses will be retained under OAE. While parabolic responders show a physiologically understandable parabolic type of dose response, positioning the TA : DIC values where the thresholds occur is also highly species-specific and potentially uncertain, meaning that it might depend on other environmental factors.

With respect to the coccolithophores, we note that this was the only group where data compilation on calcification rate across the group was possible because the OA studies were conducted in a more uniform way, using similar approaches and reporting the result in the same units. When

data for *E. huxleyi* across the comparable studies were compiled (Barcelos e Ramos et al., 2010; Fiorini et al., 2011; Iglesias-Rodrigues et al., 2008; Sciandra et al., 2003; Stoll et al., 2012; Richier et al., 2011), a significant parabolic response was obtained (Table 1), although the goodness of fit was fairly low ($R^2 = 0.16$). Despite lower R^2, we decided to use the compiled dataset because of the increased statistical power. The parabolic response obtained aligns with Langer et al. (2006) and also with the parabolic-type responses found in the synthesis studies by Paul and Bach (2020) and Bach et al. (2015). The threshold indicates the mechanisms of coccolithophore growth that are driven by CO_2, which is shown to decline with alkalinity addition. The threshold based on all studies for *E. huxleyi* combined was positioned at a TA : DIC of 1.46 ($\Omega_{ar} = 13.65$, see Table 2), which would be triggered at $850\,\mu mol\,kg^{-1}$ of added NaOH and at a pCO_2 of $60\,\mu atm$. Comparatively with the phytoplanktonic diatoms, such growth limitation is predicted at a pCO_2 amount at $100\,\mu atm$ (Riebesell et al., 1993). It is important to note that when these studies were analyzed individually, a mixture of different responses was observed. We emphasize the variability within the coccolithophore responses, which are species-specific and inherently related to the strain adaptation to their innate regional settings and dependent on a variety of other factors (Bach et al., 2015; Gafar and Schultz, 2018), including the longevity of the species, the experimental settings used in the study (e.g., nutrient-replete vs. nutrient deficient conditions), and the presence or absence of (un)suitable light conditions. Interestingly, for all the coccolithophore species other than *E. huxleyi*, responses were neutral. For validation purposes, the results of our study could not be compared, either because the calcification rates were not studied or the calcification units were not comparable (e.g., Diner et al., 2015).

4.3 Parameters impacting derivation of thresholds and their application

We developed a set of species-specific thresholds in this study, with demonstrated application across the global Ω_{ar} vs. TA : DIC conditions (Table 2; Fig. 8). The range of alkalinity additions to result in a threshold of 50 % decline in calcification rate varied significantly between the species and the type of response. The TA : DIC thresholds upon TA application ranged from 50 to $1400\,\mu mol\,kg^{-1}$ of NaOH addition and from 2250 to $6500\,\mu mol\,kg^{-1}$ of Na_2CO_3 addition, and the pH_T 9 thresholds averaged $1200\,\mu mol\,kg^{-1}$ of NaOH and $4700\,\mu mol\,kg^{-1}$ of Na_2CO_3 for all species. However, there are many parameters that impact threshold derivation and application, which we discuss in greater detail.

First, we note that differences in experimental conditions for different species make it difficult to directly compare different species' thresholds among each other. Instead, they are intended to delineate sensitivity to alkalinity addition of individual species at given experimental conditions. In the case that the lab experimental conditions mimic species' natural habitats, this threshold-related sensitivity can be extrapolated to their natural habitats.

Second, we emphasize that the threshold application should consider not only the magnitude of NaOH added, but also the duration or exposure time of the experimental study. As such, when applying the thresholds to respective model outputs or observation data, both duration and exposure time should be considered. For all the derived thresholds, we have added duration exposure information to Table 2. Additional parameters that need to be included when applying these thresholds are related to local temperature and salinity. The extracted threshold values are calculated with the temperature and salinity from the experimental conditions, which means that this threshold should not be applied to very different conditions without adjusting for salinity and temperature.

Third, we assumed global surface ocean conditions to be standardized at a pCO_2 of 425 ppm and a pH_T of 8.1 as a control point for OAE compound additions. However, we note that in different habitats, pH_T 8.1 may not represent the baseline from where OAE should be considered adding, because the average pH might be different. This means that the amount of TA required to reach a certain threshold could vary and is dependent on the baseline carbonate chemistry at the site of deployment and its variability. This is especially relevant in habitats with a lower baseline pH, where more TA would need to be added for the threshold to be reached, meaning less negative biological implications.

In addition, physical parameters of importance are related to the dilution effect, mixing, retention capacity, and the rate of the equilibration effects of the air–sea CO_2 uptake (Ferderer et al., 2022; He and Tyka, 2023; Schulz et al., 2023; Wang et al., 2023), because they determine relevant exposure duration and the variability of carbonate chemistry parameters across spatial and vertical depths. Therefore, to obtain the most accurate and regionally applicable threshold for the species of interest, it is recommended that the baseline for OAE additions be determined based on local conditions.

Lastly, if similar conditions to those induced by the OAE field trial are present in the habitats that species inhabit, it is more likely that the species might be pre-adapted to such conditions. However, if species have not been exposed to such conditions, OAE might induce rapid change in conditions and species exposure, which could be more challenging for the species. As such, it is worth considering that OAE deployments could be, at least for the most sensitive species, carried out not as a single high-dosage deployment but rather as a more continuous, lower-dosage application. This would eliminate the swings and maxima in conditions while also allowing more time for species acclimation or migration during the initial injection of the OAE deployment. Ultimately, it is the combination of all these factors that creates baseline exposure conditions that are relevant in the context of biological outcomes (Wang et al., 2023).

4.4 Direction of laboratory OAE experiments should change to incorporate field conditions

The lab OAE experiments that are being conducted right now are done under different conditions than in the field.
5 The former are conducted with the aim of gaining a wide-ranging empirical response, which implies high treatment levels of OAE additions. However, biogeochemical model outputs show that OAE-related concentrations at the injection site are high for a short time, while the realistic field
10 dosing upon rapid dilution due to mixing is low. Wang et al. (2023) reported that near-field maxima CE10 in the respective investigation area of the Bering Sea are achieved by increasing TA by about $10\,\mu\mathrm{mol\,kg}^{-1}$ in the near-field and by about $1\,\mu\mathrm{mol\,kg}^{-1}$ of NaOH in the far-field region. As
15 such, we should be more concerned about the threshold of exceedance occurring at the low NaOH dosing rather than at high NaOH additions, because these are more realistic and point to the most sensitive species. As a result, we explicitly emphasize the importance of including much lower additions
20 of TA in the experimental treatment levels to better support biological understanding and OAE application in the field. In addition, prior to the lab experiments it would be important to identify what type of response is predicted in the experimental species. This is especially pertinent for the groups for
25 which OA experimental data are limited and skewed towards the lowest TA : DIC ratio (Figs. 8, S4).

What is needed urgently for the safe biological field trial experiments is a set of protocols that are species-specific, habitat-specific, and local-conditions-specific, which would
30 allow for comprehensive and comparative risk analyses and threshold determination. As part of this, we also need to develop regionally specific indicators for biological monitoring. Ideally, such biological and environmental risk monitoring and assessment would be accompanied by the application
35 of physical mixing models with site-specific biogeochemical processes (Ho et al., 2023; Fennel et al., 2023) that can predict the maximum expected TA increase in the near-field and far-field regions of the study site, representing a more realistic exposure and better informing further experimental work.

4.5 Validating OAE responses based on the mechanistically derived calcification

This study establishes the predictions of responses that relied upon empirical experimental studies. A good alternative to validating the predicted responses is to use species-
45 specific mechanistic responses, a more accurate representation of responses compared to empirical studies. Here, we conducted a subset synthesis study for the two species of coccolithophores, using the results from this study and compared it to the literature-derived mechanistic responses where
50 the responses are described with a different set of carbonate chemistry parameters. We wanted to determine to what
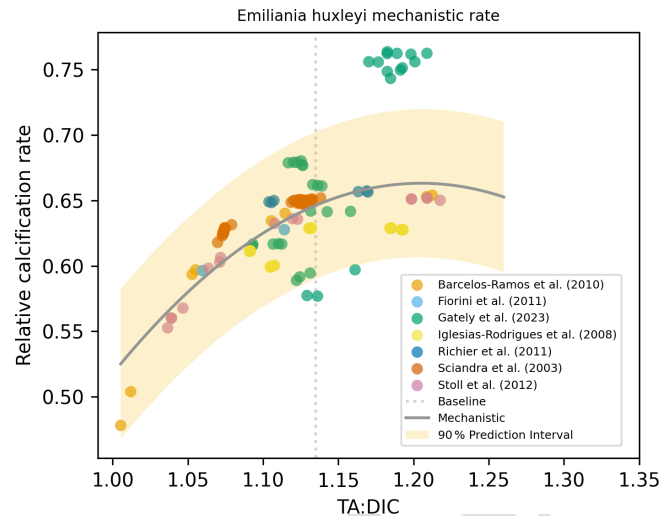
Figure 9. Mechanistic rate equation and parameters ($a = 9.56 \times 10^{-1}$, $b = 7.04 \times 10^{-4}\;\mathrm{mol\,kg}^{-1}$, $c = 2.1 \times 10^{6}\,\mathrm{kg\,mol}^{-1}$, $d = 8.27 \times 10^{6}\,\mathrm{kg\,mol}^{-1}$) taken from Bach et al. (2015) and fitted using experimental data for *E. huxleyi* (used data from the studies indicated in legend). Shading represents the 90 % prediction interval.

extent mechanistic relationships can contribute to improved, i.e., more accurate and certain, OAE predictions.

For *Emiliania huxleyi*, we used experimental TA and DIC data to calculate the $[\mathrm{HCO_3^-}]$, $[\mathrm{H^+}]$, and $[\mathrm{CO_2}]$ concentra-
55 tions to be able to use the mechanistic rate equation from Bach et al. (2015). We calculated and plotted the rate derived via a mechanistic approach and applied linear, polynomial (second-order), and exponential regressions and chose the best fit based on the lowest p value, using the same method
60 as for our experimental calcification rate data regressions. As the mechanistic rate regression based on three carbonate chemistry parameters was a parabolic fit (Bach et al., 2015), we also obtained the same fit using the experimental calcification rate data (see Fig. 9). However, when using
65 the same approach for another coccolithophore species, *Calcidiscus leptoporus* (Bach et al., 2015), our best fit did not align with the proposed mechanistic response; instead, a non-significant relationship was obtained using experimental data (Fig. S5). Such comparisons reveal species-specific relation-
70 ships are likely dependent on a lot of parameters, with one equation alone not being operable among different species from different experiments or over varied regional settings.

For most of the species, such mechanistic relationships are not available. The substrate-to-inhibitor ratio (SIR) (i.e., the
75 bicarbonate ion to hydrogen ion concentration ratio) has often been used to describe a calcification relationship based on a single parameter relationship. To see whether species rate group responses based on experimental data using TA : DIC vs. calcification rate could reproduce SIR relationships (TA :
80 DIC vs. SIR), we computed and plotted the SIR ratio. This included calculating the bicarbonate and hydrogen ion concen-

trations in CO2SYS using the experimental TA and DIC, for the mollusk, coral, and coccolithophore groups and applying a best-fit regression model. We categorized these responses (using the categories shown in Fig. 2) and compared these SIR regressions to the respective best-fit regressions based on the calcification rate responses from the experiments (shown in Table 1).

We found large differences between our calcification rate responses (based on TA : DIC vs. calcification) and the SIR-proposed mechanisms (Fig. S6). For most of the coccolithophore groups, the experimental rate regressions cannot be explained using SIR mechanisms (i.e., the responses are different). Only in the case of *Calcidiscus leptoporus* are the experimental and mechanistic responses the same (neutral). For mollusks, a third of the mechanistic rate regressions based on the SIR agreed with the experimental calcification rate regressions. The other two-thirds did not agree, especially for the studies with experimental conditions of $\Omega_{ar} > 1$. For corals, the majority of the coral species ($N = 14$) were classified as having a linear positive mechanistic relationship when using SIR relationships. When comparing this to our experimental rate regressions, we only found agreements between the experimental and mechanistic regressions in 6 out of 18 species. It seems that SIR is a less common principle of calcification and cannot be applied across a variety of species. It is likely that SIR might insufficiently explain the multitude of biological processes involved in calcification (e.g., how carbon is provisioned or the ability to regulate calcifying fluid pH). Based on these results, the consensus is that the SIR ratio might actually tend to oversimplify species' calcification rate responses. Ninokawa et al. (2024) and Li et al. (2023) emphasized that using only one parameter to describe the calcification process is insufficient and strongly recommended using at least two parameters for more accurate calcification predictions. Our findings agree with Ninokawa et al. (2024); for example, we observe that using SIR relationships to successfully describe calcification was limited to only a few species and that there are no generalizable patterns that could be applicable across multiple groups.

Mechanistic models can offer better insights into calcification responses for some species, especially when multiple environmental factors are accounted for, but they are not generally applicable across taxa. Species-specific responses are influenced by unique biological and physiological factors, which can lead to significant deviations between mechanistic and empirical predictions. Therefore, mechanistic approaches will only provide valuable frameworks for species with well-understood calcification processes. However, for many species covered in this study, the calcification process is not well-understood. By comparing mechanistic studies with experimental data, we hoped to validate the predictive results of our experimental studies. This clearly delineates a major gap in the mechanistic understanding of calcification so far, the lack of which significantly limits our ability to predict ecological and biogeochemical responses to OAE.

As such, more research is urgently needed on broader mechanistic understanding of calcification across different species; additionally, one-parameter calcification processes should be replaced with more accurate and comprehensive methods using two or three parameters.

4.6 Unknowns about ecological and biogeochemical implications call for the precautionary approach

The value of calcification as the response proxy is indicative of organismal fitness, which directly relates to OAE effects as harmful or beneficial for the species. From an ecological perspective, a total of 26.0 % negative responders demonstrate a potential for negative implications. In addition, we note that this study did not include diatoms in the analyses, which are predicted to be negatively impacted by carbonate-based OAE (Ferderer et al., 2022), leading to possible community-based ecological shifts (Bach et al., 2019). The possibility of the ecological shifts should not be neglected given the variety of the positive responders, understudied effects of OAE in non-calcifiers and their relationship with the calcifiers through the grazing impact, and lastly, unknown and highly unpredictable indirect effects. In addition, the inferences on the neutral responders should also be taken with caution.

From a biogeochemical perspective, it is reasonable to infer that OAE will introduce changes in calcification rate across species, potentially resulting in changing the carbon export or carbonate counter pump. Species-specific responses in major carbonate producers (i.e., coccolithophores, foraminifera, and pteropods) show both negative and positive responses, which could have strong effects on biogeochemical fluxes (Riebesell et al., 2017; Bach et al., 2019). Increased calcification could result in thicker and denser shells, contributing to faster sinking and increased carbonate fluxes, while decreased calcification has the opposite effect. This could potentially induce changes to the subsurface total alkalinity at intermediate and deeper depths in the water column and dissolution at or near the seafloor (Gehlen et al., 2011) or result in potential feedback of increased CO_2 flux to the atmosphere (Gattuso et al., 2021). The full scope of ecological and biogeochemical shifts remains a high-priority topic for future investigations; until these huge uncertainties are resolved, we should exercise a precautionary principle in considering the next steps of OAE field implementations.

4.7 Potential confounding effects

This study only considered the changes in carbonate chemistry due to the addition of NaOH and Na_2CO_3. However, other OAE feedstocks contain compounds that could induce biological toxicity due to the presence of trace metals (Ni, Cu, Ca, Si; Bach et al., 2019), as well as potential negative environmental impacts due to secondary precipitation (Hartmann et al., 2023; Moras et al., 2022). This study also did not focus on the sensitivity across different life stages, even

though stage-specific sensitivities to OAE are expected based on previous OA results. Furthermore, we did include data from experimental lab and field studies that involve multiple stressors in their experimental designs. As such, an additional impact of warming, dissolved oxygen, and light intensity on the OAE-induced responses was not determined, although they could elicit different biological pathways than OAE alone or have additional confounding effects.

The synthesis of the experimental studies always includes implicit biases that are based on the published experimental studies, the range and species used, regional coverage, and heterogeneity. Important consideration is the adaptation of the species used in the experimental studies because their calcification optimum might be pre-determined based on their local habitat conditions. Given that the baseline for the OAE compound addition was chosen at the global current surface pH value, some of the thresholds might actually be lower than expected.

4.8 Applications within the existing governmental regulations and the guiding principle

Our results, especially related to the use of biological thresholds or NaOH dosing, could have wider applications, most notably with policy-management governmental regulations. For example, we calculated the amount of alkalinity addition required to reach the pH_T threshold of 9, the maximum pH allowed by the US Environmental Protection Agency for wastewater entering the coastal ocean (see United States Environmental Protection Agency, 2010). To reach this threshold, $1200\,\mu mol\,kg^{-1}$ of NaOH and $4700\,\mu mol\,kg^{-1}$ of Na_2CO_3 were required on average for all species, with the lowest threshold reached at $750\,\mu mol\,kg^{-1}$ NaOH and $2250\,\mu mol\,kg^{-1}$ of Na_2CO_3 addition for *Amphibalanus improvisus*. This is a very high concentration, and the thresholds for most of the negative responders with identified thresholds (Table 2) will be exceeded far below the regulatory standards of pH_T 9 (Table 2), especially if the exposure occurred over a duration period that matters for calcification and for the organism's physiological status. This case demonstrates a discrepancy in the current chemical pH regulation and associated biological effects, where safe biological limits are not considered, and biological harm might not be prevented. Despite the fact that achieving such a high pH through NaOH / Na_2CO_3 implementation is unlikely to occur in the field, such regulations currently do not assure a safe space for marine biota, and they need to be urgently addressed.

5 Conclusions and next steps

Sufficient certainty in predicting biological responses reduces the risks and supports safe operating space for OAE implementation and scaling up. Overall, given that almost 60 % of examined species showed non-neutral response (either positive or negative), this calls for careful implementation of OAE until the safe operational temporal and spatial scales are identified and OA mitigation measures are established. The goal of this study is to serve as a baseline for prioritizing experimental and field OAE research and to assess environmental risks. Such prioritization identifies those species for which experimental work needs to be conducted first. This would involve species with the greatest OAE-related sensitivity (negative responders), species with the greatest uncertainty in response, and the species with very strong predicted positive response that could potentially introduce a shift on the community level. In addition, it would also recognize the species for which the existing knowledge is sufficient, and there is less immediate need for the OAE experiments. We hope that all presented tools provide guidance for the practicing and regulatory communities to consider OAE field application within safe limits.

It is important to emphasize that this study is the first comprehensive synthesis of the effects of OAE. Ongoing updates and additional data would enhance its value, particularly when complemented by further experimental research. Similar datasets on OA exist for various biological parameters, including genetics, physiology, and survival data, as well as for non-calcifying organisms. This availability allows for the exploration of ecological implications and contributes to developing an ecosystem-based predictive risk assessment for OAE.

Code and data availability. TS2 No new data were generated during this study; all data were collected from previously published studies. The compiled data are currently available on request. The Python code used for computing baselines per species, conceptually adding alkalinity in the form of NaOH and Na_2CO_3, predicting calcification rate response, visualizing data, and computing thresholds is available in the GitHub repository at https://github.com/hannavdmortel/OAE_calc_responses (last access: 1 November 2024) and is archived on Zenodo at https://doi.org/10.5281/zenodo.14024442 (van de Mortel, 2024). PyCO2SYS v1.8.0 (Humphreys et al., 2022) was used to solve for the carbonate system, with software available at https://doi.org/10.5281/zenodo.3744275 (Humphreys et al., 2024).

Supplement. The supplement related to this article is available online at: https://doi.org/10.5194/bg-22-1-2025-supplement.

Author contributions. NB designed and conceptualized the research and wrote the first draft of the paper. HvdM collected and curated data, conducted formal analyses, and provided visualization. GP provided the analyses using GLODAP data and also provided visualizations and formal analyses. MGR provided formal statistical analyses and visuals. RAF and AD provided insights and sug-

gestions and generated discussions about specific parts of the paper. All have contributed to the writing of this paper.

Competing interests. The contact author has declared that none of the authors has any competing interests.

Special issue statement. This article is part of the special issue "Environmental impacts of ocean alkalinity enhancement". It is not associated with a conference.

Financial support. TS3 This research has been supported by the National Oceanic and Atmospheric Administration (grant no. mCRD 48914-2023) and Javna Agencija za Raziskovalno Dejavnost RS (grant no. J1 2468).

OR

This study was funded by the NOAA NOPP project (mCRD 48914-2023 NOAA to Andrew G. Dickson, Nina Bednaršek, and Richard A. Feely), with the title mCDR 2023: Assessing CE11 chemical and biological implications of alkalinity enhancement using carbonate salts obtained from captured CO_2 to mitigate negative effects of ocean acidification and enable mCDR. This project also fully supported Hanna van de Mortel, who worked on the project as an external consultant. This work was supported by NOAA funding from the Inflation Reduction Act and the Ocean Acidification Program (ROR ID: 100018228). NOAA's Ocean Acidification Program supports this project on behalf of the National Oceanographic Partnership Program (award no. NA23OAR0170516). Hanna van de Mortelhas also been supported by the Slovenian Research Agency (ARRS J1-2468, N1-0359). This is PMEL contribution number 5621.

Review statement. This paper was edited by Patricia Grasse and reviewed by two anonymous referees.

References

Agostini, S., Harvey, B. P., Milazzo, M., Wada, S., Kon, K., Floc'h, N., Komatsu, K., Kuroyama, M., and Hall-Spencer, J. M: Seawater carbonate chemistry and kelp densities and coral coverages at three study locations and photosynthesis and calcification of corals measured in the laboratory, PANGAEA [data set], https://doi.org/10.1594/PANGAEA.944056, 2021.

Bach, L. T. and Mackinder, L. C. M.: Experiment: Dissecting the impact of CO_2 and pH on the mechanisms of photosynthesis and calcification in the coccolithophore *Emiliania huxleyi*, PANGAEA [data set], https://doi.org/10.1594/PANGAEA.830627, 2013.

Bach, L. T., Riebesell, U., and Schulz, K. G.: Seawater carbonate chemistry, growth rate and PIC and POC production during experiments with *Emiliania huxleyi* (B92/11), PANGAEA [data set], https://doi.org/10.1594/PANGAEA.771288, 2011.

Bach, L. T., Riebesell, U., Gutowska, M. A., Federwisch, L., and Schulz, K. G.: A unifying concept of coccolithophore sensitivity to changing carbonate chemistry embedded in an ecological framework, Prog. Oceanogr., 135, 125–138, https://doi.org/10.1016/j.pocean.2015.04.012, 2015.

Bach, L. T., Gill, S. J., Rickaby, R. E., Gore, S. and Renforth, P.: CO_2 removal with enhanced weathering and ocean alkalinity enhancement: potential risks and co-benefits for marine pelagic ecosystems, Front. Clim., 1, 21 pp., https://doi.org/10.3389/fclim.2019.00007, 2019.

Barcelos e Ramos, J., Müller, M. N., and Riebesell, U.: Seawater carbonate chemistry and processes during experiments with phytoplankton *Emiliania huxleyi* (strain Bergen 2005), PANGAEA [data set], https://doi.org/10.1594/PANGAEA.736022, 2010.

Bednaršek, N., Feely, R. A., Howes, E. L., Hunt, B. P., Kessouri, F., León, P., Lischka, S., Maas, A. E., McLaughlin, K., Nezlin, N. P., and Sutula, M.: Systematic review and meta-analysis toward synthesis of thresholds of ocean acidification impacts on calcifying pteropods and interactions with warming, Front. Mar. Sci., 6, 227, https://doi.org/10.3389/fmars.2019.00227, 2019.

Bednaršek, N., Naish, K. A., Feely, R. A., Hauri, C., Kimoto, K., Hermann, A. J., Michel, C., Niemi, A., and Pilcher, D.: Integrated Assessment of Ocean Acidification Risks to Pteropods in the Northern High Latitudes: Regional Comparison of Exposure, Sensitivity and Adaptive Capacity, Front. Mar. Sci., 8, 671497, https://doi.org/10.3389/FMARS.2021.671497, 2021a.

Bednaršek, N., Ambrose, R., Calosi, P., Childers, R. K., Feely, R. A., Litvin, S. Y., Long, W. C., Spicer, J. I., Štrus, J., Taylor, J., and Kessouri, F.: Synthesis of thresholds of ocean acidification impacts on decapods, Front. Mar. Sci., 8, 651102, https://doi.org/10.3389/fmars.2021.651102, 2021b.

Bednaršek, N., Calosi, P., Feely, R. A., Ambrose, R., Byrne, M., Chan, K. Y. K., Dupont, S., Padilla-Gamiño, J. L., Spicer, J. I., Kessouri, F., and Roethler, M.: Synthesis of thresholds of ocean acidification impacts on echinoderms, Front. Mar. Sci., 8, 602601, https://doi.org/10.3389/fmars.2021.602601, 2021c.

Bibby, R., Cleall-Harding, P., Rundle, S., Widdicombe, S., and Spicer, J. I.: Seawater carbonate chemistry during experiments with *Littorina littorea*, PANGAEA [data set], https://doi.org/10.1594/PANGAEA.716837, 2007.

Bove, C. B., Whitehead, R. F., and Szmant, A. M.: Seawater carbonate chemistry and gastrovascular cavity pH, calcification of *Montastraea cavernosa* and *Duncanopsammia axifuga*, PANGAEA [data set], https://doi.org/10.1594/PANGAEA.927310, 2020.

Brading, P., Warner, M. E., Davey, P., Smith, D. J., Achterberg, E. P., and Suggett, D. J.: Seawater carbonate chemistry and growth rate during experiments with phylotypes

of *Symbiodinium* (Dinophyceae), PANGAEA [data set], https://doi.org/10.1594/PANGAEA.771293, 2011.

Briggs, A. A. and Carpenter, R. C.: Seawater carbonate chemistry and photosynthesis and photochemical efficiency of *Porolithon onkodes*, PANGAEA [data set], https://doi.org/10.1594/PANGAEA.920025, 2019.

Brown, K. T., Mello-Athayde, M. A., Sampayo, E. M., Chai, A., Dove, S., and Barott, K. L.: Seawater carbonate chemistry and endosymbiont density, photosynthesis and net calcification rates of reef-building coral *Pocillopora damicornis*, PANGAEA [data set], https://doi.org/10.1594/PANGAEA.953058, 2022.

Cameron, L. P., Reymond, C. E., Müller-Lundin, F., Westfield, I. T., Grabowski, J. H., Westphal, H., and Ries, J. B.: Seawater carbonate chemistry and physiology and extrapallial fluid pH, calcification rate, and condition factor of the king scallop *Pecten maximus*, PANGAEA [data set], https://doi.org/10.1594/PANGAEA.919939, 2019.

Camp, E. F., Nitschke, M. R., Rodolfo-Metalpa, R., Houlbrèque, F., Gardner, S. G., Smith, D. J., Zampighi, M., and Suggett, D. J.: Seawater carbonate chemistry and calcification rate, net photosynthesis and respiration rate of reef-building corals, PANGAEA [data set], https://doi.org/10.1594/PANGAEA.880242, 2017.

Casareto, B. E., Niraula, M. P., Fujimura, H., and Suzuki, Y.: Seawater carbonate chemistry, primary production, biomass and calcification of plankton and bacteria, PANGAEA [data set], https://doi.org/10.1594/PANGAEA.756687, 2009.

Comeau, S., Gorsky, G., Jeffree, R., Teyssié, J.-L., and Gattuso, J.-P.: Seawater carbonate chemistry, shell linear extension and calcification during calcein staining and 45Ca experiments with pteropod *Limacina helicina*, PANGAEA [data set], https://doi.org/10.1594/PANGAEA.726856, 2009.

Comeau, S., Jeffree, R., Teyssié, J.-L., and Gattuso, J.-P.: Seawater carbonate chemistry and biological processes during experiments with *Limacina helicina*, PANGAEA [data set], https://doi.org/10.1594/PANGAEA.744720, 2010a.

Comeau, S., Gorsky, G., Alliouane, S., and Gattuso, J.-P.: Seawater carbonate chemistry and shell length of Mediterranean pteropod *Cavolinia inflexa* larvae during experiments. Laboratoire d'Océanographie de Villefranche, PANGAEA [data set], https://doi.org/10.1594/PANGAEA.733905, 2010b.

Comeau, S., Edmunds, P. J., Spindel, N. B., and Carpenter, R. C.: The responses of eight coral reef calcifiers to increasing partial pressure of CO_2 do not exhibit a tipping point, PANGAEA [data set], https://doi.org/10.1594/PANGAEA.833687, 2013.

Comeau, S., Cornwall, C. E., De Carlo, E. H., Krieger, E., and McCulloch, M. T.: Seawater carbonate chemistry and calcification physiology data in coral reef taxa, PANGAEA [data set], https://doi.org/10.1594/PANGAEA.892655, 2018.

Comeau, S., Cornwall, C. E., Pupier, C. A., DeCarlo, Thomas M., Alessi, C., Trehern, R., and McCulloch, M. T.: Seawater carbonate chemistry and calcification rate, calcifying fluid pH, calcifying fluid DIC, photosynthetic rates, metabolic alteration of pH in the DBL of corals and coralline algae, PANGAEA [data set], https://doi.org/10.1594/PANGAEA.914328, 2019.

Cornwall, C. E., Comeau, S., DeCarlo, T. M., Moore, B., D'Alexis, Q., and McCulloch, M. T.: Seawater carbonate chemistry and resistance of corals and coralline algae to ocean acidification, PANGAEA [data set], https://doi.org/10.1594/PANGAEA.914886, 2018.

Courtney, T. and Ries, J. B.: Impact of atmospheric pCO$_2$, seawater temperature, and calcification rate on the delta ^{18}O and delta ^{13}C composition of echinoid calcite (*Echinometra viridis*), PANGAEA [data set], https://doi.org/10.1594/PANGAEA.862558, 2015.

Courtney, T., Westfield, I. T., and Ries, J. B.: Seawater carbonate chemistry and calcification in the tropical urchin *Echinometra viridis* in a laboratory experiment, PANGAEA [data set], https://doi.org/10.1594/PANGAEA.824707, 2013.

Cripps, G., Widdicombe, S., Spicer, J. I. and Findlay, H. S.: Biological impacts of enhanced alkalinity in *Carcinus maenas*, Mar. Poll. Bull., 71, 190–198, https://doi.org/10.1016/j.marpolbul.2013.03.015, 2013

Dickson, A. G.: Standard potential of the reaction: $AgCl(s) + 12H_2(g) = Ag(s) + HCl(aq)$, and the standard acidity constant of the ion HSO_4^- in synthetic sea water from 273.15 to 318.15 K, J. Chem. Thermodyn., 22, 113–127, https://doi.org/10.1016/0021-9614(90)90074-z, 1990.

Diner, R. E., Benner, I., Passow, U., Iglesias-Rodriguez, M. D., and Robertson, D. L.: Negative effects of ocean acidification on calcification vary within the coccolithophore genus *Calcidiscus*, Mar. Biol., 162, 1287–1305, https://doi.org/10.1007/s00227-015-2669-x, 2015.

Eisaman, M. D., Geilert, S., Renforth, P., Bastianini, L., Campbell, J., Dale, A. W., Foteinis, S., Grasse, P., Hawrot, O., Löscher, C. R., Rau, G. H., and Rønning, J.: Assessing the technical aspects of ocean-alkalinity-enhancement approaches, in: Guide to Best Practices in Ocean Alkalinity Enhancement Research, edited by: Oschlies, A., Stevenson, A., Bach, L. T., Fennel, K., Rickaby, R. E. M., Satterfield, T., Webb, R., and Gattuso, J.-P., Copernicus Publications, State Planet, 2-oae2023, 3, https://doi.org/10.5194/sp-2-oae2023-3-2023, 2023.

Evensen, N. R. and Edmunds, P. J.: Interactive effects of ocean acidification and neighboring corals on the growth of *Pocillopora verrucosa*, PANGAEA [data set], https://doi.org/10.1594/PANGAEA.867268, 2016.

Feely, R. A., Sabine, C. L., Lee, K., Berelson, W., Kleypas, J., Fabry, V. J., and Millero, F. J. : Impact of anthropogenic CO_2 on the $CaCO_3$ system in the oceans, Science, 305, 362–366, https://doi.org/10.1126/SCIENCE.1097329, 2004.

Fennel, K., Long, M. C., Algar, C., Carter, B., Keller, D., Laurent, A., Mattern, J. P., Musgrave, R., Oschlies, A., Ostiguy, J., Palter, J. B., and Whitt, D. B.: Modelling considerations for research on ocean alkalinity enhancement (OAE), in: Guide to Best Practices in Ocean Alkalinity Enhancement Research, edited by: Oschlies, A., Stevenson, A., Bach, L. T., Fennel, K., Rickaby, R. E. M., Satterfield, T., Webb, R., and Gattuso, J.-P., Copernicus Publications, State Planet, 2-oae2023, 9, https://doi.org/10.5194/sp-2-oae2023-9-2023, 2023.

Ferderer, A., Chase, Z., Kennedy, F., Schulz, K. G., and Bach, L. T.: Assessing the influence of ocean alkalinity enhancement on a coastal phytoplankton community, Biogeosciences, 19, 5375–5399, https://doi.org/10.5194/bg-19-5375-2022, 2022.

Findlay, H. S., Kendall, M. A., Spicer, J. I., and Widdicombe, S.: Seawater carbonate chemistry and biological processes during experiments with barnacle *Semibalanus balanoides*, PANGAEA [data set], https://doi.org/10.1594/PANGAEA.737438, 2010.

Fiorini, S., Middelburg, J. J., and Gattuso, J.-P.: Seawater carbonate chemistry, nutrients, particulate carbon and growth rate of

Emiliania huxleyi (AC472), *Calcidiscus leptoporus* (AC370) and *Syracosphaera pulchra* (AC418) during experiments, PANGAEA [data set], https://doi.org/10.1594/PANGAEA.773860, 2011.

Friedlingstein, P., O'Sullivan, M., Jones, M. W., Andrew, R. M., Gregor, L., Hauck, J., Le Quéré, C., Luijkx, I. T., Olsen, A., Peters, G. P., Peters, W., Pongratz, J., Schwingshackl, C., Sitch, S., Canadell, J. G., Ciais, P., Jackson, R. B., Alin, S. R., Alkama, R., Arneth, A., Arora, V. K., Bates, N. R., Becker, M., Bellouin, N., Bittig, H. C., Bopp, L., Chevallier, F., Chini, L. P., Cronin, M., Evans, W., Falk, S., Feely, R. A., Gasser, T., Gehlen, M., Gkritzalis, T., Gloege, L., Grassi, G., Gruber, N., Gürses, Ö., Harris, I., Hefner, M., Houghton, R. A., Hurtt, G. C., Iida, Y., Ilyina, T., Jain, A. K., Jersild, A., Kadono, K., Kato, E., Kennedy, D., Klein Goldewijk, K., Knauer, J., Korsbakken, J. I., Landschützer, P., Lefèvre, N., Lindsay, K., Liu, J., Liu, Z., Marland, G., Mayot, N., McGrath, M. J., Metzl, N., Monacci, N. M., Munro, D. R., Nakaoka, S.-I., Niwa, Y., O'Brien, K., Ono, T., Palmer, P. I., Pan, N., Pierrot, D., Pocock, K., Poulter, B., Resplandy, L., Robertson, E., Rödenbeck, C., Rodriguez, C., Rosan, T. M., Schwinger, J., Séférian, R., Shutler, J. D., Skjelvan, I., Steinhoff, T., Sun, Q., Sutton, A. J., Sweeney, C., Takao, S., Tanhua, T., Tans, P. P., Tian, X., Tian, H., Tilbrook, B., Tsujino, H., Tubiello, F., van der Werf, G. R., Walker, A. P., Wanninkhof, R., Whitehead, C., Willstrand Wranne, A., Wright, R., Yuan, W., Yue, C., Yue, X., Zaehle, S., Zeng, J., and Zheng, B.: Global Carbon Budget 2022, Earth Syst. Sci. Data, 14, 4811–4900, https://doi.org/10.5194/essd-14-4811-2022, 2022.

Gafar, N. A. and Schulz, K. G.: A three-dimensional niche comparison of *Emiliania huxleyi* and *Gephyrocapsa oceanica*: reconciling observations with projections, Biogeosciences, 15, 3541–3560, https://doi.org/10.5194/bg-15-3541-2018, 2018.

Garilli, V., Rodolfo-Metalpa, R., Scuderi, D., Brusca, L., Parrinello, D., Rastrick, S. P. S., Foggo, A., Twitchett, R. J., Hall-Spencer, J. M., and Milazzo, M.: Physiological advantages of dwarfing in surviving extinctions in high-CO_2 oceans, PANGAEA [data set]. https://doi.org/10.1594/PANGAEA.847397, 2015.

Gattuso, J. P., Magnan, A. K., Bopp, L., Cheung, W. W., Duarte, C. M., Hinkel, J., Mcleod, E., Micheli, F., Oschlies, A., Williamson, P., and Billé, R.: Ocean solutions to address climate change and its effects on marine ecosystems, Front. Mar. Sci., 5, 410554, https://doi.org/10.3389/fmars.2018.00337, 2018.

Gattuso, J. P., Williamson, P., Duarte, C. M., and Magnan, A. K.: The potential for ocean-based climate action: negative emissions technologies and beyond, Front. Clim., 2, 575716, https://doi.org/10.3389/fclim.2020.575716, 2021.

Gazeau, F., Quiblier, C., Jansen, J. M., Gattuso, J.-P., Middelburg, J. J., and Heip, C. H. R.: Seawater carbonate chemistry and calcification during incubation experiments with *Mytilus edulis* and *Grassostrea gigas*, PANGAEA [data set], https://doi.org/10.1594/PANGAEA.718130, 2007.

Gazeau, F., Alliouane, S., Bock, C., Bramanti, L., López Correa, M., Gentile, M., Hirse, T., Pörtner, H.-O., and Ziveri, P.: Impact of ocean acidification and warming on the Mediterranean mussel (Mytilus galloprovincialis), PANGAEA [data set], https://doi.org/10.1594/PANGAEA.843969, 2014.

Gehlen, M., Gruber, N., Gangstø, R., Bopp, L., and Oschlies, A.: Biogeochemical consequences of ocean acidification and feedback to the earth system, Ocean Acidification, 1, 230–248, https://doi./10.1093/oso/9780199591091.003.0017, 2011.

Hansen, P. J.: Effect of high pH on the growth and survival of marine phytoplankton: implications for species succession, Aquat. Microb. Ecol., 28, 279–288, https://doi.org/10.3354/ame028279, 2002.

Hansen, P. J., Lundholm, N., and Rost, B.: Seawater carbonate chemistry and growth rate during experiments with dinoflagellates, PANGAEA [data set], https://doi.org/10.1594/PANGAEA.718182, 2007.

Hartmann, J., Suitner, N., Lim, C., Schneider, J., Marín-Samper, L., Arístegui, J., Renforth, P., Taucher, J., and Riebesell, U.: Stability of alkalinity in ocean alkalinity enhancement (OAE) approaches – consequences for durability of CO_2 storage, Biogeosciences, 20, 781–802, https://doi.org/10.5194/bg-20-781-2023, 2023.

He, J. and Tyka, M. D.: Limits and CO_2 equilibration of near-coast alkalinity enhancement, Biogeosciences, 20, 27–43, https://doi.org/10.5194/bg-20-27-2023, 2023.

Ho, D. T., Bopp, L., Palter, J. B., Long, M. C., Boyd, P. W., Neukermans, G., and Bach, L. T.: Monitoring, reporting, and verification for ocean alkalinity enhancement, State Planet, 2, 1–12, https://doi.org/10.5194/sp-2-oae2023-12-2023, 2023.

Humphreys, M. P., Lewis, E. R., Sharp, J. D., and Pierrot, D.: PyCO2SYS v1.8: marine carbonate system calculations in Python, Geosci. Model Dev., 15, 15–43, https://doi.org/10.5194/gmd-15-15-2022, 2022.

Humphreys, M. P., Schiller, A. J., Sandborn, D., Gregor, L., Pierrot, D., van Heuven, S. M. A. C., Lewis, E. R., and Wallace, D. W. R.: PyCO2SYS: marine carbonate system calculations in Python (v1.8.3.3), Zenodo [software], https://doi.org/10.5281/zenodo.13759753, 2024.

Iglesias-Rodriguez, M. D., Halloran, P. R., Rickaby, R. E. M., Hall, I. R., Colmenero-Hidalgo, E., Gittins, J. R., Green, D. R. H., Tyrrell, T., Gibbs S. J., von Dassow, P., Rehm, E., Armbrust, E. V., and Boessenkool, K. P.: Seawater carbonate chemistry and processes during experiments with *Emiliania huxleyi*, PANGAEA [data set], https://doi.org/10.1594/PANGAEA.718841, 2008.

Johnson, M. D., Bravo, L., Lucey, N. M., and Altieri, A. H.: Seawater carbonate chemistry and calcification rate of crustose coralline algae, PANGAEA [data set], https://doi.org/10.1594/PANGAEA.939809, 2021.

Keul, N., Langer, G., de Nooijer, L. J., and Bijma, J.: Seawater carbonate chemistry and benthic foraminifera *Ammonia* sp. mass, size, and growth rate during experiments, PANGAEA [data set], https://doi.org/10.1594/PANGAEA.821209, 2013.

Kheshgi, H. S.: Sequestering atmospheric carbon dioxide by increasing ocean alkalinity, Energy, 20, 915–922, 1995.

Kisakürek, B., Eisenhauer, A., Böhm, F., Hathorne, E. C., and Erez, J.: Seawater carbonate chemistry and biological processes of foraminifera, *Globigerinoides ruber* and *Globigerinella siphonifera* during experiments, PANGAEA [data set], https://doi.org/10.1594/PANGAEA.763297, 2011.

Kroeker, K. J., Kordas, R. L., Crim, R., Hendriks, I. E., Ramajo, L., Singh, G. S., Duarte, C. M., and Gattuso, J. P.: Impacts of ocean acidification on marine organisms: quantifying sensitivities and interaction with warming, Glob. Change Biol., 19, 1884–1896, https://doi.org/10.1111/gcb.12179, 2013.

Krueger, T., Horwitz, N., Bodin, J., Giovani, Maria-Evangelia, Escrig, S., Meibom, A., and Fine, M.: Seawater carbonate chemistry and photosynthesis, respiration and calcification of common reef-building coral in the Northern Red Sea, PANGAEA [data set], https://doi.org/10.1594/PANGAEA.880318, 2017.

Langer, G. and Bode, M.: Seawater carbonate chemistry, growth rate and morphology of *Calcidiscus leptoporus* (RCC1135) during experiments, PANGAEA [data set], https://doi.org/10.1594/PANGAEA.763286, 2011.

Langer, G., Geisen, M., Baumann, Karl-Heinz, Kläs, J., Riebesell, U., Thoms, S., and Young, J.: Seawater carbonate chemistry, growth rate and processes during experiments with *Coccolithus pelagicus* and *Calcidiscus leptoporus*, PANGAEA [data set], https://doi.org/10.1594/PANGAEA.721107, 2006.

Leung, J. Y., Zhang, S., and Connell, S. D.: Is ocean acidification really a threat to marine calcifiers? A systematic review and meta-analysis of 980+ studies spanning two decades, Small, 18, 2107407, https://doi.org/10.1002/smll.202107407, 2022.

Li, J., Xue, S., and Mao, Y.: Seawater carbonate parameters function differently in affecting embryonic development and calcification in Pacific abalone (Haliotis discus hannai), Aquat. Toxicol., 257, 106450, https://doi.org/10.1016/j.aquatox.2023.106450, 2023.

Lischka, S. and Riebesell, U.: Synergistic effects of ocean acidification and warming on overwintering pteropods in the Arctic, PANGAEA [data set], https://doi.org/10.1594/PANGAEA.832422, 2012.

Lischka, S., Büdenbender, J., Boxhammer, T., and Riebesell, U.: Seawater carbonate chemistry and biological processes of *Limacina helicina* during experiments, PANGAEA [data set], https://doi.org/10.1594/PANGAEA.761910, 2011.

Lutier, M., Di Poi, C., Gazeau, F., Appolis, A., Luyer, J. L., and Pernet, F.: Revisiting tolerance to ocean acidification: Insights from a new framework combining physiological and molecular tipping points of Pacific oyster, Glob. Change Biol., 28, 3333–3348. https://doi.org/10.1111/gcb.16101, 2022.

Maier, C., Hegeman, J., Weinbauer, M. G., and Gattuso, J.-P.: Seawater carbonate chemistry and calcification of *Lophelia pertusa* during experiments, PANGAEA [data set], https://doi.org/10.1594/PANGAEA.767577, 2009.

Manno, C., Morata, N., and Bellerby, R. G. J.: Seawater carbonate chemistry, survival rate, shell size, calcification rate of the planktonic foraminifer *Neogloboquadrina pachyderma* (sinistral) in a laboratory experiment, PANGAEA [data set], https://doi.org/10.1594/PANGAEA.830908, 2012.

Manríquez, P. H., Jara, M. E., Seguel, M. E., Torres, R., Alarcon, E., Lee, M. R., and Dam, H. G.: Ocean acidification and increased temperature have both positive and negative effects on early ontogenetic traits of a rocky shore keystone predator species, PANGAEA [data set], https://doi.org/10.1594/PANGAEA.869291, 2016.

Mekkes, L., Renema, W., Alin, S. R., Feely, R. A., Huisman, J., Roessingh, P., and Peijnenburg, K. T. C. A.: Seawater carbonate chemistry and shell thickness, shell dissolution of *Limacina helicina* pteropods, PANGAEA [data set], https://doi.org/10.1594/PANGAEA.930065, 2021.

Meyer, F. W., Vogel, N., Teichberg, M., Uthicke, S., Wild, C., and Diaz-Pulido, G.: The physiological response of two green calcifying algae from the great barrier reef towards high dissolved inorganic and organic carbon (DIC and DOC) availability, PAN-GAEA [data set], https://doi.org/10.1594/PANGAEA.868094, 2015.

Meyer, F. W., Vogel, N., Diele, K., Kunzmann, A., Uthicke, S., and Wild, C.: Effects of high dissolved inorganic and organic carbon availability on the physiology of the hard coral *Acropora millepora* from the Great Barrier Reef, PANGAEA [data set], https://doi.org/10.1594/PANGAEA.869416, 2016.

Monserrat, M., Comeau, S., Verdura, J., Alliouane, S., Spennato, G., Priouzeau, F., Romero, G., and Mangialajo, L.: Seawater carbonate chemistry and the recruitment of macroalgal marine forests, PANGAEA [data set], https://doi.org/10.1594/PANGAEA.955425, 2022.

Moras, C. A., Bach, L. T., Cyronak, T., Joannes-Boyau, R., and Schulz, K. G.: Ocean alkalinity enhancement–avoiding runaway $CaCO_3$ precipitation during quick and hydrated lime dissolution, Biogeosciences, 19, 3537–3557, https://doi.org/10.5194/bg-19-3537-2022, 2022.

National Academies of Sciences, Engineering, and Medicine: A research strategy for ocean-based carbon dioxide removal and sequestration, Washington, DC, The National Academies Press, https://doi.org/10.17226/26278, 2021.

Ninokawa, A., Takeshita, Y., Jellison, B. M., Jurgens, L. J., and Gaylord, B.: Seawater carbonate chemistry and mussel respiration and calcification rates, PANGAEA [data set], https://doi.org/10.1594/PANGAEA.915978, 2020.

Ninokawa, A. T., Saley, A. M., Shalchi, R., and Gaylord, B.: Multiple carbonate system parameters independently govern shell formation in a marine mussel, Commun. Earth Environ., 5, 273, https://doi.org/10.1038/s43247-024-01440-5, 2024.

Noisette, F., Bordeyne, F., Davoult, D., and Martin, S.: Assessing the physiological responses of the gastropod *Crepidula fornicata* to predicted ocean acidification and warming, PANGAEA [data set], https://doi.org/10.1594/PANGAEA.860508, 2016.

Okazaki, R., Swart, P. K., and Langdon, C.: Stress-tolerant corals of Florida Bay are vulnerable to ocean acidification, PANGAEA [data set], https://doi.org/10.1594/PANGAEA.833005, 2013.

Ong, E. Z., Briffa, M., Moens, T., and Van Colen, C.: Seawater carbonate chemistry and respiration, clearance and calcification rates of the common cockle Cerastoderma edule, PANGAEA [data set], https://doi.org/10.1594/PANGAEA.949749, 2017.

Oron, S., Evans, D., Abramovich, S., Almogi-Labin, A., and Erez, J.: Seawater carbonate chemistry and calcification, respiration, and photosynthesis of the widespread diatom-bearing LBF *Operculina ammonoides*, PANGAEA [data set], https://doi.org/10.1594/PANGAEA.929866, 2020.

Oschlies, A., Bach, L. T., Rickaby, R. E. M., Satterfield, T., Webb, R., and Gattuso, J.-P.: Climate targets, carbon dioxide removal, and the potential role of ocean alkalinity enhancement, in: Guide to Best Practices in Ocean Alkalinity Enhancement Research, edited by: Oschlies, A., Stevenson, A., Bach, L. T., Fennel, K., Rickaby, R. E. M., Satterfield, T., Webb, R., and Gattuso, J.-P., Copernicus Publications, State Planet, 2-oae2023, 1, https://doi.org/10.5194/sp-2-oae2023-1-2023, 2023.

Palmer, R. M.: Alkalinity enhancement, thermal stress and their impacts on the physiology of three Caribbean coral species: *Acropora Cervicornis, Pseudodiploria strigosa and Siderastrea siderea*, in: University of Miami, https://scholarship.miami.edu/esploro/ (last access: 6 April 2024), 2022.

Pansch, C., Schaub, I., Havenhand, J. N., and Wahl, M.: Habitat traits and food availability determine the response of marine invertebrates to ocean acidification, PANGAEA [data set], https://doi.org/10.1594/PANGAEA.831428, 2014.

Paul, A. J. and Bach, L. T.: Universal response pattern of phytoplankton growth rates to increasing CO_2, New Phytol., 228, 1710–1716, https://doi.org/10.1111/nph.16806, 2020.

Prazeres, M., Uthicke, S., and Pandolfi, J. M.: Ocean acidification induces biochemical and morphological changes in the calcification process of large benthic foraminifera, PANGAEA [data set], https://doi.org/10.1594/PANGAEA.848419, 2015.

Putnam, H. M. and Gates, R. D.: Preconditioning in the reef-building coral Pocillopora damicornis and the potential for trans-generational acclimatization in coral larvae under future climate change conditions, PANGAEA [data set], https://doi.org/10.1594/PANGAEA.859356, 2015.

Ramajo, L., Marbà, N., Prado, L., Peron, S., Lardies, M. A., Rodriguez-Navarro, A., Vargas, C. A., Lagos, N. A., and Duarte, C. M.: Biomineralization changes with food supply confer juvenile scallops (*Argopecten purpuratus*) resistance to ocean acidification, PANGAEA [data set], https://doi.org/10.1594/PANGAEA.860506, 2016.

Renforth, P. and Henderson, G.: Assessing ocean alkalinity for carbon sequestration, Rev. Geophys., 55, 636–674, https://doi.org/10.1002/2016RG000533, 2017.

Reymond, C. E., Lloyd, A., Kline, D. I., Dove, S., and Pandolfi, J. M.: Decline in growth of foraminifer *Marginopora rossi* under eutrophication and ocean acidification scenarios, PANGAEA [data set], https://doi.org/10.1594/PANGAEA.833683, 2013.

Richardson, K., Steffen, W., Lucht, W., Bendtsen, J., Cornell, S. E., Donges, J. F., Drüke, M., Fetzer, I., Bala, G., von Bloh, W., and Feulner, G.: Earth beyond six of nine planetary boundaries, Sci. Adv., 9, 2458, https://doi.org/10.1126/sciadv.adh2458, 2023.

Richier, S., Fiorini, S., Kerros, Marie-Emmanuelle, von Dassow, P., and Gattuso, J.-P.: Seawater carbonate chemistry, particulate inorganic and organic carbon and growth rate of *Emiliana huxleyi* (RCC1216) during experiments, PANGAEA [data set], https://doi.org/10.1594/PANGAEA.770439, 2011.

Riebesell, U. and Gattuso, J. P.: Lessons learned from ocean acidification research, Nat. Clim. Change, 5, 12–14, https://doi.org/10.1038/nclimate2456, 2015.

Riebesell, U., Wolf-Gladrow, D. A., and Smetacek, V.: Carbon dioxide limitation of marine phytoplankton growth rates, Nature, 361, 249–251, https://doi.org/10.1038/361249a0, 1993.

Riebesell, U., Bach, L. T., Bellerby, R. G., Monsalve, J. R. B., Boxhammer, T., Czerny, J., Larsen, A., Ludwig, A., and Schulz, K. G.: Competitive fitness of a predominant pelagic calcifier impaired by ocean acidification, Nat. Geosci., 10, 19–23, https://doi.org/10.1038/ngeo2854, 2017.

Ries, J. B.: A physicochemical framework for interpreting the biological calcification response to CO_2-induced ocean acidification. Geochim. Cosmochim. Ac., 75, 4053–4064, https://doi.org/10.1016/j.gca.2011.04.025, 2011.

Ries, J. B., Cohen, A. L., and McCorkle, D. C.: Seawater carbonate chemistry and biological processes during experiments with calcifying organisms, PANGAEA [data set], https://doi.org/10.1594/PANGAEA.733947, 2009.

Sett, S., Bach, L. T., Schulz, K. G., Koch-Klavsen, S., Lebrato, M., and Riebesell, U.: Temperature modulates coccolithophorid sensitivity of growth, photosynthesis and calcification to increasing seawater pCO_2, PANGAEA [data set], https://doi.org/10.1594/PANGAEA.835214, 2014.

Schulz, K. G., Bach, L. T., and Dickson, A. G.: Seawater carbonate chemistry considerations for ocean alkalinity enhancement research: theory, measurements, and calculations, in: Guide to Best Practices in Ocean Alkalinity Enhancement Research, edited by: Oschlies, A., Stevenson, A., Bach, L. T., Fennel, K., Rickaby, R. E. M., Satterfield, T., Webb, R., and Gattuso, J.-P., Copernicus Publications, State Planet, 2-oae2023, 2, https://doi.org/10.5194/sp-2-oae2023-2-2023, 2023.

Sciandra, A., Harlay, J., Lefèvre, D., Lemee, R., Rimmelin, P., Denis, M., and Gattuso, J.-P.: Seawater carbonate chemistry and processes during experiments with *Emiliania huxleyi* (TW1), PANGAEA [data set], https://doi.org/10.1594/PANGAEA.727841, 2003.

Seabold, S. and Perktold, J.: Statsmodels: Econometric and statistical modeling with Python, in: 9th Python in Science Conference, 57–61, Austin, TX, 28 June–3 July 2010, https://doi.org/10.25080/Majora-92bf1922-011, 2010.

Sinutok, S., Hill, R., Doblin, M. A., Wuhrer, R., and Ralph, P. J.: Seawater carbonate chemistry, calcification rate, oxygen production, maximum quantum yield, symbiont density, chlorophyll concentration and crystal width of *Halimeda macroloba, Halimeda cylindracea* and *Marginopora vertebralis* during experiments, PANGAEA [data set], https://doi.org/10.1594/PANGAEA.774792, 2011.

Sordo, L., Duarte, C., Joaquim, S., Gaspar, M. B., and Matias, D.: Seawater carbonate chemistry and growth and survival of juveniles of the striped venus clam *Chamelea gallina*, PANGAEA [data set], https://doi.org/10.1594/PANGAEA.937477, 2021.

Stoll, H. M., Cruzado, A., Shimizu, N., and Kanamaru, K. : Seawater carbonate chemistry and B/Ca, calcification rate of Emiliania huxleyi and Coccolithus braarudii, PANGAEA [data set], https://doi.org/10.1594/PANGAEA.949913, 2012.

Sulpis, O., Lauvset, S. K., and Hagens, M.: Current estimates of K_1^* and K_2^* appear inconsistent with measured CO_2 system parameters in cold oceanic regions, Ocean Sci., 16, 847–862, https://doi.org/10.5194/os-16-847-2020, 2020.

Tatters, A. O., Schnetzer, A., Fu, F., Lie, A. Y. A., Caron, D. A., and Hutchins, D. A.: Short- versus long-term responses to changing CO_2 in a coastal dinoflagellate bloom, PANGAEA [data set], https://doi.org/10.1594/PANGAEA.823381, 2013.

Truchot, J.: Water carbonate alkalinity as a determinant of hemolymph acid-base balance in the shore crab, *Carcinus maenas*: a study at two different ambient PCO_2 and PO_2 levels, J. Comp. Physiol. B, 154, 601–606, https://doi.org/10.1007/bf00684414, 1984.

Truchot, J.: Changes in the Hemolymph Acid-Base State of the Shore Crab, *Carcinus maenas*, Exposed to Simulated Tidepool Conditions, Biol. Bull., 170, 506–518, https://doi.org/10.2307/1541858, 1986.

United States Environmental Protection Agency (EPA): National Pollutant Discharge Elimination System (NPDES) Permit Writers' Manual, U.S. Environmental Protection Agency, Washington, D.C., https://www.epa.gov/npdes/npdes-permit-writers-manual (last access: TS4), 2010.

Uppström, L. R.: The boron / chlorinity ratio of deep-sea water from the Pacific Ocean, Deep-Sea Res., 21, 161–162, https://doi.org/10.1016/0011-7471(74)90074-6, 1974.

Uthicke, S. and Fabricius, K. E.: Seawater carbonate chemistry, productivity and calcification of Marginopora vertebralis in a laboratory experiment, PANGAEA [data set], https://doi.org/10.1594/PANGAEA.831207, 2012.

van de Mortel, H.: hannavdmortel/OAE_calc_responses: Temperature change + pre-industrial lines removed (v1.1.0), Zenodo [code], https://doi.org/10.5281/zenodo.14024442, 2024.

Van de Waal, D. B., John, U., Ziveri, P., Reichart, Gert-Jan, Hoins, M., Sluijs, A., and Rost, B.: Seawater carbonate chemistry and growth, calcification of *Thoracosphaera heimii* in a laboratory experiment, PANGAEA [data set], https://doi.org/10.1594/PANGAEA.824705, 2013.

Vásquez-Elizondo, R. M. and Enríquez, S.: Coralline algal physiology is more adversely affected by elevated temperature than reduced pH, PANGAEA [data set], https://doi.org/10.1594/PANGAEA.860802, 2016.

Waldbusser, G. G., Voigt, E. P., Bergschneider, H., Green, M. A., and Newell, R. I. E.: Seawater carbonate chemistry and calcification rate of eastern oyster Crassostrea virginica, PANGAEA [data set], https://doi.org/10.1594/PANGAEA.758181, 2011.

Wang, H., Pilcher, D. J., Kearney, K. A., Cross, J. N., Shugart, O. M., Eisaman, M. D., and Carter, B. R. Simulated impact of ocean alkalinity enhancement on atmospheric CO_2 removal in the Bering Sea, Earth's Future, 11, e2022EF002816, https://doi.org/10.1029/2022EF002816, 2023.

Wang, X., Feng, X., Zhuang, Y., Lu, J., Wang, Y., Gonçalves, R. J., Li, X., Lou, Y., and Guan, W.: Seawater carbonate chemistry and physiology and toxicity of dinoflagellate *Karenia mikimotoi*, PANGAEA [data set], https://doi.org/10.1594/PANGAEA.923683, 2019.

White, M. M., Drapeau, D. T., Lubelczyk, L. C., Abel, V. C., Bowler, B. C., and Balch, W. M.: Seawater carbonate chemistry and calcification of an estuarine coccolithophore, PANGAEA [data set], https://doi.org/10.1594/PANGAEA.923623, 2018.

Xue, L. and Cai, W. J.: Total alkalinity minus dissolved inorganic carbon as a proxy for deciphering ocean acidification mechanisms, Mar. Chem., 222, 103791, https://doi.org/10.1016/j.marchem.2020.103791, 2020.

Zhang, M., Fang, J., Zhang, J., Li, B., Ren, S., Mao, Y., and Gao, Y.: Seawater carbonate chemistry and calcification and respiration of Chlamys farreri, PANGAEA [data set], https://doi.org/10.1594/PANGAEA.949604, 2011.

Remarks from the language copy-editor

CE1   Please give an explanation of why this needs to be changed. We have to ask the handling editor for approval. Thanks.
CE2   Please note a comma was removed here.
CE3   Please note the slight adjustments.
CE4   Please note the slight adjustments.
CE5   Please give an explanation of why this needs to be changed. We have to ask the handling editor for approval. Thanks.
CE6   Please give an explanation of why this needs to be changed. We have to ask the handling editor for approval. Thanks.
CE7   Please give an explanation of why this needs to be changed. We have to ask the handling editor for approval. Thanks.
CE8   Please give an explanation of why this needs to be changed. We have to ask the handling editor for approval. Thanks.
CE9   Please give an explanation of why this needs to be changed. We have to ask the handling editor for approval. Thanks.
CE10   Please double-check this sentence, as adjustments might be necessary.
CE11   Please double-check the name of this project, including capitalization.

Remarks from the typesetter

TS1   Adjusted to our house standards.
TS2   Please confirm new section name.
TS3   Please note that the financial support section you have inserted differs from the funder information you provided during submission. Please check which funder information is correct and provide an updated text. Please also double-check your acknowledgements to see whether repeated information can be removed or changed accordingly. Thanks.
TS4   Please provide date of last access (day month year).